CHAPTER

Flight in a Non-steady Atmosphere 14

14.1 The influence of atmospheric disturbances on flying qualities

All of the material in the previous chapters is based on the assumption of a quasi-steady atmosphere. However, in reality the atmosphere is anything but steady and it is frequently necessary to assess the likely impact of atmospheric disturbances on aircraft flying qualities. In general, flight in a non-steady atmosphere will make it more difficult for the pilot to carry out his mission task, leading to an increase in workload and consequent degradation in *level* of flying qualities. The perceived nature of this degradation will depend on the stability and control properties of the aircraft, the type of atmospheric disturbance, the disturbance intensity, and the way in which the disturbance excites the flight dynamics.

From a flying qualities perspective, atmospheric disturbances are treated as involuntary inputs to the aircraft that give rise to unwanted response. Clearly, the response dynamics depend totally on the dynamic properties of the airframe and the "shape" and intensity of the atmospheric disturbance. In every situation there exists a limit on the severity of the atmospheric disturbance that can be tolerated, and the degree of tolerance can, to an extent, be designed into an aircraft by tailoring its dynamic properties and by capitalising on the attenuating properties of a stability augmentation system. Today it is also common practice to incorporate explicit gust alleviation features into the flight control systems of advanced technology aeroplanes to alleviate structural loading in particular. Thus all aircraft design, flight control system design, and flight dynamics analysis which address the problems of flight in a non-steady atmosphere must have access to appropriate disturbance models, together with the essential tools and techniques for conducting flight dynamics assessment. The intention here is to set out a summary of the common models, tools, and techniques used in flight dynamics analysis.

Whenever the flying qualities of aircraft in the presence of atmospheric disturbances are under review, the specific flight dynamics concerns are

- Increase in pilot workload
- Degradation in flight path control
- Degradation in ride quality
- Influence on structural integrity
- Erosion of flight control system authority margins

It is therefore a requirement to evaluate aircraft and flight control system behaviour in representative non-steady atmospheric flight conditions. Comprehensive flying qualities requirements and their means of compliance are set out in detail in MIL-F-8785C (1980), MIL-STD-1797A (1987), and Def-Stan 00-970 (2011). Much of the following material is derived from these standards.

Table 14.1 Correlation between Level of Flying Qualities and Atmospheric Disturbance Intensity

Level of Flying Qualities	Atmospheric Disturbance Intensity			
	Light	**Moderate**	**Severe**	**Extreme**
1	Flying qualities adequate for mission	Flying qualities adequate for mission, but with increase in pilot workload and/or degradation in mission effectiveness	Flying qualities adequate for safe control, but with excessive pilot workload and/or inadequate mission effectiveness	Flying qualities sufficient to maintain control to fly out of disturbance
2	Flying qualities adequate for mission, but with increase in pilot workload and/or degradation in mission effectiveness	Flying qualities adequate for safe control, but with excessive pilot workload and/or inadequate mission effectiveness	Flying qualities sufficient to maintain control to fly out of disturbance	Flying qualities sufficient to recover control after upset
3	Flying qualities adequate for safe control, but with excessive pilot workload and/or inadequate mission effectiveness	Flying qualities sufficient to maintain control to fly out of disturbance	Flying qualities sufficient to recover control after upset	No requirement

A rationale for the formal flying qualities requirements is expressed in MIL-STD-1797A: "To provide a rational means for specifying the allowable degradation in flying qualities in the presence of increased intensities of atmospheric disturbances." This may be interpreted as the means for *quantifying* the effects of flight in the presence of atmospheric disturbances in terms of the apparent degradation in *Level* of flying qualities.

The key parameter in any consideration of flight in the presence of atmospheric disturbances is the disturbance intensity, and four descriptors are universally used: *light*, *moderate*, *severe*, and *extreme*. All of the requirements documents provide a definition of *atmospheric disturbance intensity* and its correlation with *Level* of flying qualities. A useful definition is given by Hoh et al. (1982), which provides the basis for the definitions given in MIL-STD-1797A (see Table 14.1).

14.2 Methods of evaluation

Two methods are used for the evaluation of aircraft response to atmospheric disturbance in the engineering domain. By far the most common method involves the use of continuous simulation models, where the disturbance velocity components are generated synthetically by, for example, filtering white noise and summing the resulting turbulent air velocities with the aircraft velocity components. This modifies the aircraft's velocity, angle of attack, and angle of sideslip, changing the forces and moments acting on the aircraft and thus producing output response time histories which are then evaluated visually, or by suitable signal processing software or by pilot opinion rating in the piloted flight simulator context. Alternatively, for formal analytical evaluation, frequency

response methods are used to assess, for example, the magnitude and *root mean square* (rms) intensity of the motion variables of interest. Again, the disturbances are modelled in the frequency domain by filtering white noise using transfer functions. In most cases, assessment is concerned with the intensity of acceleration response to atmospheric disturbances, as this has significance for aircraft handling, for structural loading, and for passenger ride comfort.

In all evaluation methods it is important that the atmospheric disturbance models be sufficiently simple to allow meaningful simulation or analysis. To this end it is helpful if the parameters used to describe the atmosphere models have some relationship, or relevance, to the interpretation of aircraft dynamics and flying qualities. In other words, in the formulation of complex atmospheric disturbance models it is necessary to achieve a balance between engineering convenience and physical correctness. Thus, as in many things aeronautical, a compromise is the outcome.

14.3 Atmospheric disturbances

All atmospheric disturbances are defined by their *temporal* characteristics, *spatial* characteristics, and energy content or *intensity*. The apparent magnitude of those characteristics is also dependent on the size and shape of the aircraft, the speed at which it encounters the disturbances, and the altitude. Clearly, an adequate description for mathematical modelling is difficult to quantify, and it becomes necessary to simplify the descriptions to representative but manageable definitions. The four most commonly used models of atmospheric disturbances are *steady wind*, *wind shear*, *discrete gusts*, and *continuous turbulence*, all of which are realistic atmospheric features which tend to occur in combination during flight, depending on local conditions. A summary of each of these, as found in the flying qualities requirements documents, is contained in the following paragraphs.

14.3.1 Steady wind

A steady wind is continuous and assumed to act parallel to the surface of the earth; the principal cases of interest are head wind, tail wind, and crosswind during take-off and landing. Steady wind effects can be balanced out by thrust and the aircraft's flying control surfaces and thus do not normally define a flying qualities problem with the exception of a crosswind. In particular, a crosswind constitutes a potential hazard during take-off and landing when it acts across the runway, and an increasingly strong crosswind requires increasing amounts of rudder and aileron deflection to balance the wind-induced moments. Hence, all aircraft have limits for operation in the presence of crosswind and, for the purposes of flying qualities analysis, typical requirements are given in Table 14.2.

Table 14.2 Crosswind Intensity

Intensity	Reference Value (knots)
Light	0–10
Moderate	11–30
Severe	31–45

14.3.2 Wind shear

Wind shear is defined as a time rate of change in wind speed and direction lasting for 10 seconds or more, the assumption being that shears of less than 10 seconds are unlikely to constitute a flying qualities hazard. See, for example Hoh et al. (1982), which includes a useful discussion of wind shear in the context of flying qualities requirements.

As for steady wind, wind shear presents a problem during take-off and landing and, when encountered, the aircraft will rise or sink according to the relative direction and magnitude of the wind velocity gradient. Since the effect of wind shear on the aircraft is to cause an upset in normal acceleration, the requirements quantify the wind shear limits in terms of acceleration response as given in Table 14.3, where subscript γ_{max} is the maximum power climb angle and subscript γ_{min} is the flight idle glide angle.

Table 14.3 Wind Shear Intensity

Wind Shear	Reference Normal Acceleration
Decreasing headwind	$g_{\gamma_{max}} \leq 1.0\ m/s^2\ (3.4\ ft/s^2)$
Decreasing tailwind	$g_{\gamma_{min}} \leq 0.5\ m/s^2\ (1.7\ ft/s^2)$

14.3.3 Discrete gusts

A discrete gust is a single disturbance event and is usually assumed to be embedded in continuous turbulence. Gusts occur randomly, and their magnitude and duration are usually correlated with the properties of continuous turbulence. Therefore, their definition derives from the definition of continuous turbulence.

14.3.4 Continuous turbulence

Continuous turbulence comprises random disturbances that are observed to occur in *patches* of varying *scale* and *intensity*. Most aeronautical engineers agree on what turbulence is, but agreement on how to describe and quantify turbulence models for use in flying qualities analysis is rather more subjective, and opinions differ.

The scale of continuous turbulence is generally determined by the overall magnitude of its effect on aircraft response. Not surprisingly, the scale is defined by the size of the patch of turbulence and by the velocity of the aircraft as it traverses the patch. When the scale is large and the application is concerned with flying and handling qualities analysis, the effects are assumed to act uniformly over the whole airframe. This is interpreted to mean that the disturbance velocities may be taken to act at, or about, the *cg* of the aircraft. This is the simplest interpretation and is certainly the easiest to model. However, when the scale is small it is more appropriate that the disturbances should be variously distributed over the airframe, and this poses an altogether more difficult problem. See, for example, the paper by Thomasson (2000) in which the equations of motion for a vehicle subject to distributed fluid disturbances are developed.

Turbulence intensity quantifies the energy content of the disturbance and is usually defined in terms of the rms value σ_g over the turbulence frequency spectrum. Since turbulence is modelled as

Table 14.4 Gust and Turbulence Intensity

Intensity	Reference rms Velocity σ_g (m/s)
Light	0.9 (3 ft/s)
Moderate	1.8 (6 ft/s)
Severe	3.7 (12 ft/s)
Extreme	7.3 (24 ft/s)

a velocity disturbance, it is reduced to three linear velocity components and three angular velocity components. The velocity components are known to be correlated to an extent, but since the degree of correlation is not fully understood it is usual practice to assume that the velocity components are uncorrelated. The principal component is regarded as the rms horizontal "gust" velocity, and this is used to quantify the turbulence intensity and from which of all velocity components are derived. Typical rms gust and turbulence intensity is defined in Table 14.4.

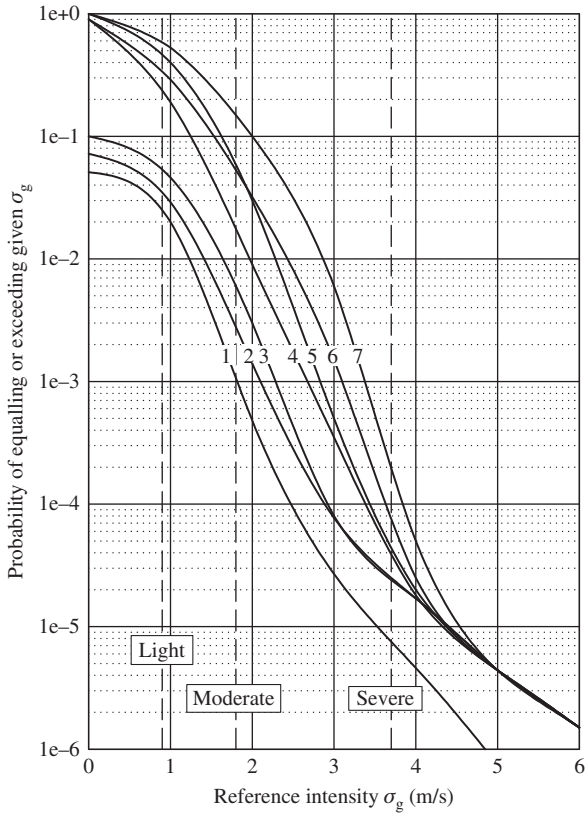

FIGURE 14.1 Probability of equalling or exceeding a given turbulence reference intensity at specific altitudes.

Broadly, altitude influences the scale of the turbulence and the probability of encountering atmospheric disturbances of a given intensity. At low altitude, where terrain has a significant effect, encounters with disturbances are more frequent; also, the scale of the turbulence is smaller and it includes earth boundary layer effects. At high altitude, encounters with disturbances are less frequent, the scale of turbulence is larger, there is greater homogeneity within patches, and it includes clear air turbulence effects.

The probability of encountering turbulence of a given intensity has been the subject of much research and debate. The American model is similar in general, but differs from the UK model in detail. The reasons for the differences arise because the models are empirical and derived from independent experimental flight research. For example, a substantial programme of flight experiments was undertaken in the United Kingdom in the 1960s and 1970s by the Royal Aircraft Establishment and resulted in the description of what is believed to be a more representative empirical turbulence model. Reference to this work may be found in Jones (1973), and the model provides the basis for the requirements in Def-Stan 00-970. Opinions among experts differ, of course, but most importantly the flying qualities requirements in Def-Stan 00-970 and in MIL-F-8785C share a high degree of numerical conformity. The gust and turbulence intensity model given in Def-Stan 00-970 is reproduced as Fig. 14.1, and the *light*, *moderate*, and *severe* turbulence boundaries are superimposed as indicated. The plots shown in Fig. 14.1 are altitude-dependent, as shown in Table 14.5.

Below an altitude of 75 m, the turbulence reference intensity is taken as constant and may be defined by the values given in Table 14.4. Note in Fig. 14.1 that a step in the high-altitude plots (1−3) occurs at $\sigma_g = 0$; the explanation for this phenomenon is based on the assumption of "*a finite probability of conditions existing with zero turbulence reference intensity*".

Table 14.5 Gust and Turbulence Altitude Dependency

Plot	Altitude	
1	15,000 m (50,000 ft)	
2	9,000 m (30,000 ft)	
3	3,000 m (10,000 ft)	
4	300 m (1000 ft)	Above flat terrain
5	300 m (1000 ft)	Above hilly terrain
6	≤ 75 m (≤250 ft)	Above flat terrain
7	≤ 75 m (≤250 ft)	Above hilly terrain

14.4 Extension of the linear aircraft equations of motion

Atmospheric disturbances are represented by and introduced into the aircraft equations of motion as linear and angular velocity components. Since it is usual to assume that the aircraft is in straight and level flight when it encounters a horizontal patch of turbulence, the disturbance velocity components are referred to the earth axes reference frame. When applying the disturbance velocity components to the equations of motion, it is common practice to refer them directly to aircraft

body axes, without transformation, on the basis that the disturbances are small enough to be regarded as small perturbations and that in level flight the aircraft attitudes are also small angles. However, when evaluating aircraft response to gusts and turbulence at low altitude, below ~ 50 m, it is considered good practice to transform the disburbance velocity components into aircraft axes. The forces and moments due to atmospheric disturbances are introduced to the equations of motion in the manner described in the development of equations (4.20). Since atmospheric disturbances are quantified as velocity disturbances, their effect on the aircraft is determined by the aerodynamic response to linear and angular velocity perturbations and, for linear small-perturbation models, enter the equations of motion via the aerodynamic stability derivatives.

Considering rigid body aircraft response to gusts and turbulence only—that is, when structural modes responses are considered insignificant and omitted from the analysis—the effect on the aircraft is assumed to comprise uniform immersion in the disturbance field and exposure to the linear gradients of the disturbance velocity components as the aircraft traverses the field. Thus the uniform immersion in the gust and turbulence field leads to the assumption that the velocity components u_g, v_g, and w_g act at the aircraft cg and that positive velocity disturbances act along the aircraft reference axes in the positive sense. The total impact of each of the gust velocity components on the aircraft is modelled with a Taylor series expansion comprising the linear term acting at the cg and a series of linear velocity gradient terms. All except the first derivative terms are assumed to be negligible and are omitted from the model. The remaining linear gradients of the disturbance velocity components with distance, as the aircraft traverses the patch of turbulence, give rise to angular velocity response, p_g, q_g, and r_g about the aircraft axes. As before, assume that the aircraft is in steady level flight when it traverses the horizontal patch of turbulence and that the disturbance perturbations are small. Thus, at coordinates $(x,y,0)$ referred to aircraft body axes, the components of angular velocity due to the linear velocity components acting at the cg are given approximately by

$$p_g = -\frac{\partial w_g}{\partial y} \quad q_g = \frac{\partial w_g}{\partial x} \quad r_g = -\frac{\partial v_g}{\partial x} \tag{14.1}$$

Now,

$$q_g = \frac{\partial w_g}{\partial x} = -\frac{\partial w_g}{\partial t}\frac{\partial t}{\partial x} = -\dot{w}_g \frac{1}{U_e} \tag{14.2}$$

Whence, approximately,

$$\dot{w}_g = -q_g U_e \tag{14.3}$$

14.4.1 Disturbed body incidence and sideslip

Normal gusts and lateral gusts give rise to disturbances in body incidence and sideslip, respectively. These disturbances can be evaluated by means of a simple analysis of the disturbed flow geometry, and knowledge of the estimated values of incidence α_g and sideslip β_g, due to gusts, enables direct estimates of the forces and moments acting on the aircraft in response to atmospheric disturbances. Clearly, this has benefits for estimation of the impact of atmospheric disturbances on the performance, stability, control, and flying qualities of an aircraft without first having to set up and solve the equations of motion.

In steady level flight in an undisturbed atmosphere, the total velocity of the aircraft is given by

$$V_0 = \sqrt{U_e^2 + V_e^2 + W_e^2} \tag{14.4}$$

and in straight flight the steady lateral component of velocity $V_e = 0$. With reference to Section 2.4.1, it is easily shown that steady body incidence and steady sideslip angles are given by

$$\alpha_e = \tan^{-1}\frac{W_e}{U_e} \quad \beta_e = \sin^{-1}\frac{V_e}{V_0} \tag{14.5}$$

In disturbed flight, let the gust velocity components be (u_g, v_g, w_g); then equations (14.4) and (14.5) become

$$\begin{aligned} V &= \sqrt{(U_e + u_g)^2 + (V_e + v_g)^2 + (W_e + w_g)^2} \\ \alpha &= \tan^{-1}\left(\frac{W_e + w_g}{U_e + u_g}\right) \\ \beta &= \sin^{-1}\left(\frac{V_e + v_g}{V}\right) \end{aligned} \tag{14.6}$$

Equations (14.6) may be simplified by treating the gust velocity components as small perturbations about steady flight, such that the usual approximations may be applied. Thus

$$U_e >> u_g \quad U_e \cong V_0 \quad V \cong V_0$$

and

$$\begin{aligned} \alpha &= \alpha_e + \alpha_g \cong \tan^{-1}\left(\frac{W_e + w_g}{V_0}\right) \cong \frac{W_e + w_g}{V_0} = \frac{W_e}{V_0} + \frac{w_g}{V_0} \\ \beta &= \beta_e + \beta_g \cong \sin^{-1}\left(\frac{V_e + v_g}{V_0}\right) \cong \frac{V_e + v_g}{V_0} = \frac{V_e}{V_0} + \frac{v_g}{V_0} \end{aligned} \tag{14.7}$$

It is therefore seen from equations (14.7) that

$$\alpha_g \cong \frac{w_g}{V_0} \quad \text{and} \quad \beta_g \cong \frac{v_g}{V_0} \tag{14.8}$$

14.4.2 The longitudinal equations of motion

The development of the longitudinal equations of motion (4.40), which for the most general case are referred to aircraft body axes, may be written to include the gust and turbulence velocity components. It is important to recognise that the aerodynamic contributions to the equations of motion are determined with respect to the disturbed air mass, and, in accordance with the notation, the dimensional equations (4.40) may be expanded to

$$
\begin{aligned}
m\dot{u} - \overset{\circ}{X}_u(u-u_g) - \overset{\circ}{X}_{\dot{w}}(\dot{w}-\dot{w}_g) - \overset{\circ}{X}_w(w-w_g) - \overset{\circ}{X}_q(q-q_g) + mW_e q + mg\cos\theta_e &= \overset{\circ}{X}_\eta\,\eta + \overset{\circ}{X}_\tau\,\tau \\
-\overset{\circ}{Z}_u(u-u_g) + m\dot{w} - \overset{\circ}{Z}_{\dot{w}}(\dot{w}-\dot{w}_g) - \overset{\circ}{Z}_w(w-w_g) - \overset{\circ}{Z}_q(q-q_g) - mU_e q + mg\sin\theta_e &= \overset{\circ}{Z}_\eta\,\eta + \overset{\circ}{Z}_\tau\,\tau \\
-\overset{\circ}{M}_u(u-u_g) - \overset{\circ}{M}_{\dot{w}}(\dot{w}-\dot{w}_g) - \overset{\circ}{M}_w(w-w_g) + I_y\dot{q} - \overset{\circ}{M}_q(q-q_g) &= \overset{\circ}{M}_\eta\,\eta + \overset{\circ}{M}_\tau\,\tau
\end{aligned}
\tag{14.9}
$$

Making the substitution for $\dot{w}_g$ from equation (14.3), equations (14.9) may be rearranged in state-space form:

$$
\begin{bmatrix} m & -\overset{\circ}{X}_{\dot{w}} & 0 & 0 \\ 0 & m-\overset{\circ}{Z}_{\dot{w}} & 0 & 0 \\ 0 & -\overset{\circ}{M}_{\dot{w}} & I_y & 0 \\ 0 & 0 & 0 & 1 \end{bmatrix} \begin{bmatrix} \dot{u} \\ \dot{w} \\ \dot{q} \\ \dot{\theta} \end{bmatrix} = \begin{bmatrix} \overset{\circ}{X}_u & \overset{\circ}{X}_w & \overset{\circ}{X}_q - mW_e & -mg\cos\theta_e \\ \overset{\circ}{Z}_u & \overset{\circ}{Z}_w & \overset{\circ}{Z}_q + mU_e & -mg\sin\theta_e \\ \overset{\circ}{M}_u & \overset{\circ}{M}_w & \overset{\circ}{M}_q & 0 \\ 0 & 0 & 1 & 0 \end{bmatrix} \begin{bmatrix} u \\ w \\ q \\ \theta \end{bmatrix}
$$
$$
+ \begin{bmatrix} \overset{\circ}{X}_\eta & \overset{\circ}{X}_\tau \\ \overset{\circ}{Z}_\eta & \overset{\circ}{Z}_\tau \\ \overset{\circ}{M}_\eta & \overset{\circ}{M}_\tau \\ 0 & 0 \end{bmatrix} \begin{bmatrix} \eta \\ \tau \end{bmatrix} + \begin{bmatrix} -\overset{\circ}{X}_u & -\overset{\circ}{X}_w & -\overset{\circ}{X}_q + \overset{\circ}{X}_{\dot{w}}U_e \\ -\overset{\circ}{Z}_u & -\overset{\circ}{Z}_w & -\overset{\circ}{Z}_q + \overset{\circ}{Z}_{\dot{w}}U_e \\ -\overset{\circ}{M}_u & -\overset{\circ}{M}_w & -\overset{\circ}{M}_q + \overset{\circ}{M}_{\dot{w}}U_e \\ 0 & 0 & 0 \end{bmatrix} \begin{bmatrix} u_g \\ w_g \\ q_g \end{bmatrix}
\tag{14.10}
$$

or

$$
\mathbf{M}\dot{\mathbf{x}} = \mathbf{A}'\mathbf{x} + \mathbf{B}'\mathbf{u} + \mathbf{E}'\mathbf{u}_g \tag{14.11}
$$

where it is seen that the disturbance terms simply appear as additional inputs to the equations through the gust input matrix $\mathbf{E}'$ and the gust velocity vector $\mathbf{u}_g$. Alternatively, the equations of motion may be written in concise state-space form by multiplying equations (14.10) by the inverse of the mass matrix $\mathbf{M}$, with reference to the definitions of the concise derivatives given in Table A2.5 in Appendix 2, to give

$$
\begin{bmatrix} \dot{u} \\ \dot{w} \\ \dot{q} \\ \dot{\theta} \end{bmatrix} = \begin{bmatrix} x_u & x_w & x_q & x_\theta \\ z_u & z_w & z_q & z_\theta \\ m_u & m_w & m_q & z_\theta \\ 0 & 0 & 1 & 0 \end{bmatrix} \begin{bmatrix} u \\ w \\ q \\ \theta \end{bmatrix} + \begin{bmatrix} x_\eta & x_\tau \\ x_\eta & x_\tau \\ x_\eta & x_\tau \\ 0 & 0 \end{bmatrix} \begin{bmatrix} \eta \\ \tau \end{bmatrix} + \left[\begin{array}{cc|c} -x_u & -x_w & -x_q - W_e + \dfrac{2\overset{\circ}{X}_{\dot{w}}U_e}{\left(m-\overset{\circ}{Z}_{\dot{w}}\right)} \\ \hline -z_u & -z_w & -z_q + \dfrac{U_e\left(m+\overset{\circ}{Z}_{\dot{w}}\right)}{\left(m-\overset{\circ}{Z}_{\dot{w}}\right)} \\ \hline -m_u & -m_w & -m_q + \dfrac{2m\overset{\circ}{M}_{\dot{w}}U_e}{I_y\left(m-\overset{\circ}{Z}_{\dot{w}}\right)} \\ \hline 0 & 0 & 0 \end{array}\right] \begin{bmatrix} u_g \\ w_g \\ q_g \end{bmatrix}
\tag{14.12}
$$

or

$$
\dot{\mathbf{x}} = \mathbf{A}\mathbf{x} + \mathbf{B}\mathbf{u} + \mathbf{E}\mathbf{u}_g \tag{14.13}
$$

With controls **u** fixed, equation (14.12) simplifies to

$$\begin{bmatrix} \dot{u} \\ \dot{w} \\ \dot{q} \\ \dot{\theta} \end{bmatrix} = \begin{bmatrix} x_u & x_w & x_q & x_\theta \\ z_u & z_w & z_q & z_\theta \\ m_u & m_w & m_q & z_\theta \\ 0 & 0 & 1 & 0 \end{bmatrix} \begin{bmatrix} u \\ w \\ q \\ \theta \end{bmatrix} + \left[\begin{array}{c|c|c} -x_u & -x_w & -x_q - W_e + \dfrac{2\overset{\circ}{X}_{\dot{w}} U_e}{\left(m - \overset{\circ}{Z}_{\dot{w}}\right)} \\ \hline -z_u & -z_w & -z_q + \dfrac{U_e\left(m + \overset{\circ}{Z}_{\dot{w}}\right)}{\left(m - \overset{\circ}{Z}_{\dot{w}}\right)} \\ \hline -m_u & -m_w & -m_q + \dfrac{2m\overset{\circ}{M}_{\dot{w}} U_e}{I_y\left(m - \overset{\circ}{Z}_{\dot{w}}\right)} \\ \hline 0 & 0 & 0 \end{array}\right] \begin{bmatrix} u_g \\ w_g \\ q_g \end{bmatrix} \tag{14.14}$$

or, equivalently,

$$\dot{\mathbf{x}} = \mathbf{A}\mathbf{x} + \mathbf{E}\mathbf{u}_g \tag{14.15}$$

and equation (14.15) may be solved in the usual way to obtain the aircraft longitudinal gust response transfer functions.

14.4.3 The lateral-directional equations of motion

In a similar way, the dimensional lateral-directional equations of motion (4.45) for the most general case are also referred to aircraft body axes and may be written to include the gust and turbulence velocity components. Again, it is important to recognise that the aerodynamic contributions to the equations of motion are determined with respect to the disturbed air mass, and, in accordance with the notation, equations (4.45) may be written as

$$\begin{aligned} m\dot{v} - \overset{\circ}{Y}_v(v - v_g) - \overset{\circ}{Y}_p(p - p_g) + mW_e p - \overset{\circ}{Y}_r(r - r_g) - mU_e r - mg\phi\cos\theta_e - mg\psi\sin\theta_e &= \overset{\circ}{Y}_\xi \xi + \overset{\circ}{Y}_\zeta \zeta \\ -\overset{\circ}{L}_v(v - v_g) + I_x\dot{p} - \overset{\circ}{L}_p(p - p_g) - I_{xz}\dot{r} - \overset{\circ}{L}_r(r - r_g) &= \overset{\circ}{L}_\xi \xi + \overset{\circ}{L}_\zeta \zeta \\ -\overset{\circ}{N}_v(v - v_g) - I_{xz}\dot{p} - \overset{\circ}{N}_p(p - p_g) + I_z\dot{r} - \overset{\circ}{N}_r(r - r_g) &= \overset{\circ}{N}_\xi \xi + \overset{\circ}{N}_\zeta \zeta \end{aligned} \tag{14.16}$$

With reference to Table A2.7 in Appendix 2, and after some rearrangement, equations (14.16) may be written in concise state-space form as follows:

$$\begin{bmatrix} \dot{v} \\ \dot{p} \\ \dot{r} \\ \dot{\phi} \\ \dot{\psi} \end{bmatrix} = \begin{bmatrix} y_v & y_p & y_r & y_\phi & y_\psi \\ l_v & l_p & l_r & l_\phi & l_\psi \\ n_v & n_p & n_r & n_\phi & n_\psi \\ 0 & 1 & 0 & 0 & 0 \\ 0 & 0 & 1 & 0 & 0 \end{bmatrix} \begin{bmatrix} v \\ p \\ r \\ \phi \\ \psi \end{bmatrix} + \begin{bmatrix} y_\xi & y_\zeta \\ l_\xi & l_\zeta \\ n_\xi & n_\zeta \\ 0 & 0 \\ 0 & 0 \end{bmatrix} \begin{bmatrix} \xi \\ \zeta \end{bmatrix} + \begin{bmatrix} -y_v & -y_p + W_e & -y_r - U_e \\ -l_v & -l_p & -l_r \\ -n_v & -n_p & -n_r \\ 0 & 0 & 0 \\ 0 & 0 & 0 \end{bmatrix} \begin{bmatrix} v_g \\ p_g \\ r_g \end{bmatrix} \tag{14.17}$$

With controls **u** fixed, equations (14.17) simplify to

$$\begin{bmatrix} \dot{v} \\ \dot{p} \\ \dot{r} \\ \dot{\phi} \\ \dot{\psi} \end{bmatrix} = \begin{bmatrix} y_v & y_p & y_r & y_\phi & y_\psi \\ l_v & l_p & l_r & l_\phi & l_\psi \\ n_v & n_p & n_r & n_\phi & n_\psi \\ 0 & 1 & 0 & 0 & 0 \\ 0 & 0 & 1 & 0 & 0 \end{bmatrix} \begin{bmatrix} v \\ p \\ r \\ \phi \\ \psi \end{bmatrix} + \begin{bmatrix} -y_v & -y_p + W_e & -y_r - U_e \\ -l_v & -l_p & -l_r \\ -n_v & -n_p & -n_r \\ 0 & 0 & 0 \\ 0 & 0 & 0 \end{bmatrix} \begin{bmatrix} v_g \\ p_g \\ r_g \end{bmatrix} \tag{14.18}$$

14.4.4 The equations of motion for aircraft with stability augmentation

The equations of motion given above represent those of the basic unaugmented aircraft, and for both the longitudinal and lateral-directional equations of motion the generic state-space description is given by equation (14.13):

$$\dot{\mathbf{x}} = \mathbf{A}\mathbf{x} + \mathbf{B}\mathbf{u} + \mathbf{E}\mathbf{u}_g$$

All advanced technology aircraft incorporate stability and control augmentation and a typical control law (see for example Section 11.7) would take the form

$$\mathbf{u} = \mathbf{v} - \mathbf{K}\mathbf{x} \tag{14.19}$$

where **v** is a vector of input control command variables. Whence, the closed-loop equations of motion are given by substituting equation (14.19) into equation (14.13) to give

$$\dot{\mathbf{x}} = [\mathbf{A} - \mathbf{B}\mathbf{K}]\mathbf{x} + \mathbf{B}\mathbf{v} + \mathbf{E}\mathbf{u}_g \tag{14.20}$$

The output equation corresponding with the state equation (14.20) takes the general form

$$\mathbf{y} = \mathbf{C}\mathbf{x} + \mathbf{D}\mathbf{v} + \mathbf{F}\mathbf{u}_g \tag{14.21}$$

where the matrices **C**, **D**, and **F** are specified to give the desired vector of output variables **y**.

Clearly, the closed-loop aircraft gust response transfer functions, with controls **v** fixed, may be obtained by solving the following state and output equations in the usual way:

$$\begin{aligned} \dot{\mathbf{x}} &= [\mathbf{A} - \mathbf{B}\mathbf{K}]\mathbf{x} + \mathbf{E}\mathbf{u}_g \\ \mathbf{y} &= \mathbf{C}\mathbf{x} + \mathbf{F}\mathbf{u}_g \end{aligned} \tag{14.22}$$

In any analysis of aircraft response to atmospheric disturbances, in addition to observing the perturbations in the motion variables it is also of particular relevance to observe the height h response, acceleration responses a_x, a_y, and a_z measured at the cg, and normal load factor n_z response, also measured at the cg. Accordingly, it is good practice to augment equations (14.22) to include those variables using the methods described in Chapter 5.

EXAMPLE 14.1

Stability and control data for the Douglas DC-8 transport aeroplane are given by Teper (1969), and the flight condition describing the aircraft flying a holding pattern at an altitude of 15,000 ft is chosen to illustrate the procedure for obtaining the gust response transfer functions. It is convenient that the equations of motion are referred to wind, or stability, axes, thereby simplifying

the mathematical procedure. Flight condition data are given in Table 14.6, and longitudinal derivative data are given in Table 14.7 in American normalised form, the notation for which is described in Section 4.4.3.

A number of stability derivatives are sufficiently small that they are assumed to be zero—namely, $X_{\dot{w}} = Z_{\dot{w}} = X_q = Z_q \cong 0$. In accordance with the usual American notation, the velocity-dependent stability derivatives, X_u, Z_u, and M_u, represent aerodynamic effects only whereas the derivatives X_u^*, Z_u^*, and M_u^* represent the aerodynamic effects plus the effects of thrust dependency on velocity perturbations. The latter derivatives are used in the equations of motion when the engine and thrust models are not included explicitly. However, if it is known, or assumed, that atmospheric disturbances do not affect thrust, the velocity-dependent derivatives representing aerodynamic effects only, X_u, Z_u, and M_u, should be used when incorporating the gust and turbulence velocity components into the equations of motion.

The longitudinal normalised equations of motion as given, referred to wind axes and omitting zero terms, may be written as

$$\begin{aligned} \dot{u} - X_u u - X_w w + g\theta &= X_{\delta_s}\delta_s \\ -Z_u u + \dot{w} - Z_w w - V_0 q &= Z_{\delta_s}\delta_s \\ -M_u u - M_{\dot{w}}\dot{w} - M_w w + \dot{q} + M_q q &= M_{\delta_s}\delta_s \\ \dot{\theta} &= q \end{aligned} \tag{14.23}$$

Table 14.6 Douglas DC-8 Flight Condition Data

Altitude	h	15,000 ft
Mach number	M_0	0.443
Velocity	V_0	468.2 ft/s
Mass	m	5900 slugs
Moment of inertia in pitch	I_y	2,940,000 slugft^2
Trim pitch attitude	θ_e	0 deg
Gravitational constant	g	32.2 ft/s^2

Table 14.7 Normalised Stability and Control Derivatives

X_u	−0.00707 1/s	Z_{δ_s}	−23.7 ft/s^2/rad
X_u^*	−0.00714 1/s	Mu	−0.000063 1/fts
X_w	0.0321 1/s	M_u^*	−0.000063 1/fts
X_{δ_s}	0 ft/s^2/rad	Mw	−0.0107 1/fts
Z_u	−0.1329 1/s	$M_{\dot{w}}$	−0.00072 1/ft
Z_u^*	−0.1329 1/s	Mq	−0.991 1/s
Z_w	−0.756 1/s	M_{δ_s}	−3.24 1/s^2

The height and normal acceleration auxiliary equations are as follows, where in both equations w is the normal perturbation component of aircraft inertial velocity:

$$\begin{aligned} \dot{h} &= -w + V_0\theta \\ a_z &= \dot{w} - V_0 q \end{aligned} \tag{14.24}$$

In the manner of equations (14.10), equations (14.23) may be developed to include the gust velocity components, the substitution for $\dot{w}_g$ from equation (14.3) may be made, the height equation (14.24) may be incorporated for completeness, and the whole arranged in state form to give

$$\begin{bmatrix} 1 & 0 & 0 & 0 & 0 \\ 0 & 1 & 0 & 0 & 0 \\ 0 & -\mathrm{M}_{\dot{w}} & 1 & 0 & 0 \\ 0 & 0 & 0 & 1 & 0 \\ 0 & 0 & 0 & 0 & 1 \end{bmatrix} \begin{bmatrix} \dot{u} \\ \dot{w} \\ \dot{q} \\ \dot{\theta} \\ \dot{h} \end{bmatrix} = \begin{bmatrix} \mathrm{X}_u^* & \mathrm{X}_w & 0 & -g & 0 \\ \mathrm{Z}_u^* & \mathrm{Z}_w & V_0 & 0 & 0 \\ \mathrm{M}_u^* & \mathrm{M}_w & \mathrm{M}_q & 0 & 0 \\ 0 & 0 & 1 & 0 & 0 \\ 0 & -1 & 0 & V_0 & 0 \end{bmatrix} \begin{bmatrix} u \\ w \\ q \\ \theta \\ h \end{bmatrix} + \begin{bmatrix} \mathrm{X}_{\delta_s} \\ \mathrm{Z}_{\delta_s} \\ \mathrm{M}_{\delta_s} \\ 0 \\ 0 \end{bmatrix} \delta_s + \begin{bmatrix} -\mathrm{X}_u & -\mathrm{X}_w & 0 \\ -\mathrm{Z}_u & -\mathrm{Z}_w & 0 \\ -\mathrm{M}_u & -\mathrm{M}_w & -\mathrm{M}_q + \mathrm{M}_{\dot{w}} V_0 \\ 0 & 0 & 0 \\ 0 & 0 & 0 \end{bmatrix} \begin{bmatrix} u_g \\ w_g \\ q_g \end{bmatrix} \tag{14.25}$$

Substituting numerical values from Tables 14.6 and 14.7 into equations (14.25) and multiplying by the inverse of the mass matrix **M** reduces the equations to the standard concise form:

$$\begin{bmatrix} \dot{u} \\ \dot{w} \\ \dot{q} \\ \dot{\theta} \\ \dot{h} \end{bmatrix} = \begin{bmatrix} -7.14e-3 & 0.0321 & 0 & -32.2 & 0 \\ -0.1329 & -0.756 & 468.2 & 0 & 0 \\ 3.2688e-5 & -0.01016 & -1.3281 & 0 & 0 \\ 0 & 0 & 1 & 0 & 0 \\ 0 & -1 & 0 & 468.2 & 0 \end{bmatrix} \begin{bmatrix} u \\ w \\ q \\ \theta \\ h \end{bmatrix} + \begin{bmatrix} 0 \\ -23.7 \\ -3.22294 \\ 0 \\ 0 \end{bmatrix} \delta_s + \begin{bmatrix} 7.07e-3 & -0.0321 & 0 \\ 0.1329 & 0.756 & 0 \\ -3.2688e-5 & 0.01016 & 0.65896 \\ 0 & 0 & 0 \\ 0 & 0 & 0 \end{bmatrix} \begin{bmatrix} u_g \\ w_g \\ q_g \end{bmatrix} \tag{14.26}$$

The aircraft state equation relating response to gust and turbulence input disturbances is given by equation (14.15):

$$\dot{\mathbf{x}} = \mathbf{A}\mathbf{x} + \mathbf{E}\mathbf{u}_g$$

From equation (14.26), assuming controls-fixed, this may be written directly:

$$\begin{bmatrix} \dot{u} \\ \dot{w} \\ \dot{q} \\ \dot{\theta} \\ \dot{h} \end{bmatrix} = \begin{bmatrix} -7.14e-3 & 0.0321 & 0 & -32.2 & 0 \\ -0.1329 & -0.756 & 468.2 & 0 & 0 \\ 3.2688e-5 & -0.01016 & -1.3281 & 0 & 0 \\ 0 & 0 & 1 & 0 & 0 \\ 0 & -1 & 0 & 468.2 & 0 \end{bmatrix} \begin{bmatrix} u \\ w \\ q \\ \theta \\ h \end{bmatrix} + \begin{bmatrix} 7.07e-3 & -0.0321 & 0 \\ 0.1329 & 0.756 & 0 \\ -3.2688e-5 & 0.01016 & 0.65896 \\ 0 & 0 & 0 \\ 0 & 0 & 0 \end{bmatrix} \begin{bmatrix} u_g \\ w_g \\ q_g \end{bmatrix} \tag{14.27}$$

The corresponding output equation is

$$\mathbf{y} = \mathbf{C}\mathbf{x} + \mathbf{F}\mathbf{u}_g \tag{14.28}$$

It is useful to augment the output vector $\mathbf{y}$ to include normal acceleration a_z and normal load factor $n_z = -a_z/g$, as these are response variables of interest in the analysis of aircraft response to gusts and turbulence. The definition of a_z is given in equations (14.24), and the numerical description of $\dot{w}$ may be obtained from the second row of equations (14.27). In this way, the output equation (14.28) may be assembled:

$$\begin{bmatrix} u \\ w \\ q \\ \theta \\ h \\ a_z \\ n_z \end{bmatrix} = \begin{bmatrix} 1 & 0 & 0 & 0 & 0 \\ 0 & 1 & 0 & 0 & 0 \\ 0 & 0 & 1 & 0 & 0 \\ 0 & 0 & 0 & 1 & 0 \\ 0 & 0 & 0 & 0 & 1 \\ -0.1329 & -0.756 & 0 & 0 & 0 \\ 4.12733e-3 & 0.023473 & 0 & 0 & 0 \end{bmatrix} \begin{bmatrix} u \\ w \\ q \\ \theta \\ h \end{bmatrix} + \begin{bmatrix} 0 & 0 & 0 \\ 0 & 0 & 0 \\ 0 & 0 & 0 \\ 0 & 0 & 0 \\ 0 & 0 & 0 \\ 0.1329 & 0.756 & 0 \\ 4.12733e-3 & -0.023478 & 0 \end{bmatrix} \begin{bmatrix} u_g \\ w_g \\ q_g \end{bmatrix} \tag{14.29}$$

To obtain the aircraft response to a normal gust w_g disturbance, for example, equations (14.27) and (14.29) may be solved in the usual way for the single-input variable w_g. Thus, for this particular example, the state-space equations simplify to equations (14.30), which may be

solved using MATLAB, Program CC, or a similar computational tool set to obtain the gust and turbulence response transfer functions. In a similar way, the response transfer functions for u_g and q_g disturbances can be obtained by suitable adjustment of the matrices **E** and **F**:

$$\begin{aligned}
\dot{\mathbf{x}} &= \begin{bmatrix} -7.14e-3 & 0.0321 & 0 & -32.2 & 0 \\ -0.1329 & -0.756 & 468.2 & 0 & 0 \\ 3.2688e-5 & -0.01016 & -1.3281 & 0 & 0 \\ 0 & 0 & 1 & 0 & 0 \\ 0 & -1 & 0 & 468.2 & 0 \end{bmatrix} \mathbf{x} + \begin{bmatrix} -0.0321 \\ 0.756 \\ 0.01016 \\ 0 \\ 0 \end{bmatrix} \mathbf{u} \\
\mathbf{y} &= \begin{bmatrix} 1 & 0 & 0 & 0 & 0 \\ 0 & 1 & 0 & 0 & 0 \\ 0 & 0 & 1 & 0 & 0 \\ 0 & 0 & 0 & 1 & 0 \\ 0 & 0 & 0 & 0 & 1 \\ -0.1329 & -0.756 & 0 & 0 & 0 \\ 4.12733e-3 & 0.023473 & 0 & 0 & 0 \end{bmatrix} \mathbf{x} + \begin{bmatrix} 0 \\ 0 \\ 0 \\ 0 \\ 0 \\ 0.756 \\ -0.023478 \end{bmatrix} \mathbf{u}
\end{aligned} \tag{14.30}$$

where

$$\begin{aligned}
\mathbf{x}^{\mathrm{T}} &= [u \quad w \quad q \quad \theta \quad h] \\
\mathbf{u} &= w_g \\
\mathbf{y}^{\mathrm{T}} &= [u \quad w \quad q \quad \theta \quad h \quad a_z \quad n_z]
\end{aligned}$$

The solution of equations (14.30) gives the following gust response transfer functions:

$$\begin{aligned}
\frac{u(s)}{w_g(s)} &= \frac{-0.0321\,s^2(s^2+1.328\,s+10.19)}{s(s^2+0.005438\,s+0.007685)(s^2+2.086\,s+5.759)} \\
\frac{w(s)}{w_g(s)} &= \frac{0.756\,s(s+7.623)(s^2+0.0070245\,s+0.007679)}{s(s^2+0.005438\,s+0.007685)(s^2+2.086\,s+5.759)} \\
\frac{q(s)}{w_g(s)} &= \frac{0.01016\,s^3(s+0.007037)}{s(s^2+0.005438\,s+0.007685)(s^2+2.086\,s+5.759)} \ \frac{\text{rad/s}}{\text{ft/s}} \\
\frac{\theta(s)}{w_g(s)} &= \frac{0.01016\,s^2(s+0.007037)}{s(s^2+0.005438\,s+0.007685)(s^2+2.086\,s+5.759)} \ \frac{\text{rad}}{\text{ft/s}} \\
\frac{h(s)}{w_g(s)} &= \frac{-0.756(s^2-0.01916\,s+0.04304)(s+1.36)}{s(s^2+0.005438\,s+0.007685)(s^2+2.086\,s+5.759)} \ \frac{\text{ft}}{\text{ft/s}} \\
\frac{a_z(s)}{w_g(s)} &= \frac{0.756\,s^2(s^2-0.01916\,s+0.04304)(s+1.36)}{s(s^2+0.005438\,s+0.007685)(s^2+2.086\,s+5.759)} \ \frac{\text{ft/s}^2}{\text{ft/s}} \\
\frac{n_z(s)}{w_g(s)} &= \frac{-0.2348\,s^2(s^2-0.01916\,s+0.04304)(s+1.36)}{s(s^2+0.005438\,s+0.007685)(s^2+2.086\,s+5.759)} \ \frac{g}{\text{ft/s}}
\end{aligned} \tag{14.31}$$

Observation of the transfer functions (14.31) suggests that aircraft response is consistent with the flight physics associated with a positive small-perturbation disturbance in normal velocity. The stability is governed by the familiar properties of the characteristic polynomial described by the common denominator of the transfer functions. The longitudinal stability characteristics associated with the aircraft at this flight condition are

Phugoid damping ratio	$\zeta_p = 0.031$
Phugoid natural frequency	$\omega_p = 0.088$ rad/s
Short-period damping ratio	$\zeta_s = 0.435$
Short-period natural frequency	$\omega_s = 2.4$ rad/s

The pole at $s = 0$ corresponds with the height integration characteristic. The information given in Teper (1969) does not include provision for stability augmentation, so it is assumed that the aircraft is not fitted with a longitudinal autostabilisation system. The stability characteristics indicated are entirely consistent with a stable unaugmented aircraft of the late 1950s period.

It should also be noted that the height h, normal acceleration a_z, and normal load factor n_z transfer functions exhibit a significant nonminimum phase property which is entirely consistent with the adverse aerodynamic properties of a large aircraft of this type.

Finally, note that the transfer functions include up to three zeros at $s = 0$. Some of these cancel with the pole at $s = 0$, but they have not been removed from the transfer functions in this example for reasons of clarity of understanding. In the computational solution many of these poles and zeros have a small non-zero value of either sign due to rounding errors in the solution algorithm, and great care must be exercised in their interpretation. For the purpose of comparison, the author used a number of alternative algorithms to solve equations (14.30), and each solution produced small but different values for the poles and zeros which correctly sit at $s = 0$. In this kind of situation it becomes abundantly clear that a good understanding of anticipated aircraft response is essential.

14.5 Turbulence modelling

Random atmospheric disturbances are assumed to comprise continuous turbulence, with embedded discrete gusts, and subject to steady and non-steady wind effects. The disturbances are further assumed to be distributed spatially over a horizontal patch, or field, through which the aircraft flies in steady level flight. For mathematical convenience, the patch, or field of disturbances, is assumed to be stationary in time and space for the period of encounter by the aircraft. This approach to turbulence modelling is sometimes referred to as *frozen field turbulence*. The *spatial frequency* of the turbulence is denoted Ω and has units of radians per unit length, or distance. The time dependency of the response of the aircraft arises from the *frequency of encounter*, which depends on the velocity at which the aircraft traverses the patch of frozen turbulence. Thus the *temporal frequency* ω is given by

$$\omega = \Omega V_0 \quad \text{with units rad/s} \tag{14.32}$$

Considerable care is required with regard to the units used in turbulence analysis because much is assumed in the flying qualities requirements documents; also, the units most commonly used in atmospheric turbulence modelling are not always consistent with those commonly used in systems analysis using tools like MATLAB and Progam CC. Continuous random disturbances, conveniently referred to as turbulence, are characterised by the *rms intensity*, *power spectral density* (PSD), and *scale*.

14.5.1 The von Kármán model

The von Kármán model defines the power spectra of the linear velocity components of turbulence, where the spectra have a Gaussian, or normal, distribution and the model is generally considered to be the most accurate approximation of real turbulence. The power spectra of the axial u_g, lateral v_g, and normal w_g turbulence velocity components are given by

$$\Phi_{ug}(\Omega) = \sigma_{ug}^2 \frac{2\mathscr{L}_u}{\pi} \frac{1}{(1+(1.339\mathscr{L}_u\Omega)^2)^{\frac{5}{6}}} \tag{14.33}$$

$$\Phi_{vg}(\Omega) = \sigma_{vg}^2 \frac{\mathscr{L}_v}{\pi} \frac{\left(1+\frac{8}{3}(1.339\mathscr{L}_v\Omega)^2\right)}{(1+(1.339\mathscr{L}_v\Omega)^2)^{\frac{11}{6}}} \tag{14.34}$$

$$\Phi_{wg}(\Omega) = \sigma_{wg}^2 \frac{\mathscr{L}_w}{\pi} \frac{\left(1+\frac{8}{3}(1.339\mathscr{L}_w\Omega)^2\right)}{(1+(1.339\mathscr{L}_w\Omega)^2)^{\frac{11}{6}}} \tag{14.35}$$

where $\mathscr{L}_u$, $\mathscr{L}_v$, and $\mathscr{L}_w$ are the appropriate scale lengths. The units of the PSD functions given in equations (14.33), (14.34), and (14.35) are $(\text{m/s})^2/(\text{rad/m})$ or $(\text{ft/s})^2/(\text{rad/ft})$. Since the fractional indices in the denominators of the von Kármán model are mathematically difficult to implement in practical applications, the simpler but less accurate Dryden model is commonly used as an alternative.

14.5.2 The Dryden model

The Dryden turbulence model is mathematically simpler and has been developed to model both linear and angular disturbance velocity components. However, it is considered to be a less accurate although acceptable alternative to the von Kármán model for practical flight dynamics investigations. In the past, all aircraft simulation utilised analogue computing techniques and to reproduce the von Kármán turbulence model by this means was difficult in the extreme. Consequently, the Dryden model was adopted as an alternative to alleviate this problem and continues to be used extensively in the simulation environment. Modern computer tools enable both the von Kármán and the Dryden models to be reproduced in a simulation environment with equal facility and, strictly, the von Kármán turbulence model should be the model of choice. However, the Dryden model remains in common usage since it is well understood, it is easier to work with, and it has a long and established acceptability.

The Dryden power spectra of the axial u_g, lateral v_g, and normal w_g turbulence velocity components are given by

$$\Phi_{ug}(\Omega) = \sigma_{ug}^2 \frac{2\mathscr{L}_u}{\pi} \frac{1}{(1+(\mathscr{L}_u\Omega)^2)} \tag{14.36}$$

$$\Phi_{vg}(\Omega) = \sigma_{vg}^2 \frac{\mathscr{L}_v}{\pi} \frac{(1+3(\mathscr{L}_v\Omega)^2)}{(1+(\mathscr{L}_v\Omega)^2)^2} \tag{14.37}$$

$$\Phi_{wg}(\Omega) = \sigma_{wg}^2 \frac{\mathscr{L}_w}{\pi} \frac{(1+3(\mathscr{L}_w\Omega)^2)}{(1+(\mathscr{L}_w\Omega)^2)^2} \tag{14.38}$$

The units of the Dryden PSD functions are the same as those of the von Kármán functions. Additionally, the power spectra of the roll p_g, pitch q_g, and yaw r_g angular turbulence velocity components are given by

$$\Phi_{pg}(\Omega) = \frac{\sigma_{wg}^2}{\mathscr{L}_w} \frac{0.8\left(\frac{\pi\mathscr{L}_w}{4b}\right)^{\frac{1}{3}}}{\left(1+\left(\frac{4b}{\pi}\Omega\right)^2\right)} \tag{14.39}$$

$$\Phi_{qg}(\Omega) = \frac{\Phi_{wg}(\Omega)\,\Omega^2}{\left(1+\left(\frac{4b\Omega}{\pi}\right)^2\right)} \tag{14.40}$$

$$\Phi_{rg}(\Omega) = \frac{\Phi_{vg}(\Omega)\,\Omega^2}{\left(1+\left(\frac{3b\Omega}{\pi}\right)^2\right)} \tag{14.41}$$

where $\mathscr{L}_u$, $\mathscr{L}_v$, $\mathscr{L}_w$ and $\mathscr{L}_p$ are the appropriate scale lengths, and b is the wing span. Note that q_g is dependent on w_g and r_g is dependent on v_g.

The components of angular turbulence velocity are often small and are frequently ignored. A simple test to determine their relative significance is given in Hoh et al. (1982).

When

$$\left(\frac{b}{\mathscr{L}_w}\right)^{\frac{1}{2}} > \frac{L_v}{L_p} \quad \text{then} \quad p_g = 0 \tag{14.42}$$

$$\left(\frac{\pi b}{8\mathscr{L}_w}\right)^{\frac{1}{2}} > \frac{M_w}{M_q} \quad \text{then} \quad q_g = 0 \tag{14.43}$$

$$\left(\frac{\pi b}{6\mathscr{L}_v}\right)^{\frac{1}{2}} > \frac{N_v}{N_r} \quad \text{then} \quad r_g = 0 \tag{14.44}$$

It is interesting to consider the properties of the inequalities (14.42), (14.43), and (14.44). The terms on the left-hand side are functions of wing span b divided by scale length $\mathscr{L}$, and increase in magnitude as the size of the aircraft increases. The terms on the right-hand side comprise the ratio of the stiffness derivative and damping derivative in roll, pitch, and yaw, respectively. Obviously, the magnitude of the ratio diminishes as damping increases. Thus, in well-damped aeroplanes, the components of angular velocity disturbances may be attenuated to the extent that they can be

omitted from the modelling, and for very large well-damped aeroplanes the angular velocity disturbances are even more likely to be insignificant.

14.5.3 Comparison of the von Kármán and Dryden models

To illustrate the essential differences between the von Kármán and Dryden turbulence models for the axial components of velocity u_g, their power spectra are compared as given by equations (14.33) and (14.36), respectively. By multiplying each equation by the spatial frequency Ω, and with some rearrangement, the normalised power spectral density is plotted against the normalised spatial frequency as shown in Fig. 14.2.

It is evident that the spectral energy distributions for the two models are similar in shape but that the Dryden model tends to overestimate the energy content around the centre frequency and underestimate the energy content at the extreme higher frequencies of the distribution. The high frequency difference is of less concern since the aircraft rigid body dynamics naturally attenuate the effects of disturbances as the frequency increases. However, this may not be the case in the context of structural mode excitation. On the other hand, the low-frequency region of the distributions below the centre frequency is of much greater significance since the natural attenuation of the response to disturbances is generally small. Note in Fig. 14.2 that the lower-frequency distributions of the two models are in very close agreement, thereby endorsing the use of the Dryden model as a good alternative to the von Kármán model for evaluations in which the lower-frequency response to disturbances is of the greatest importance.

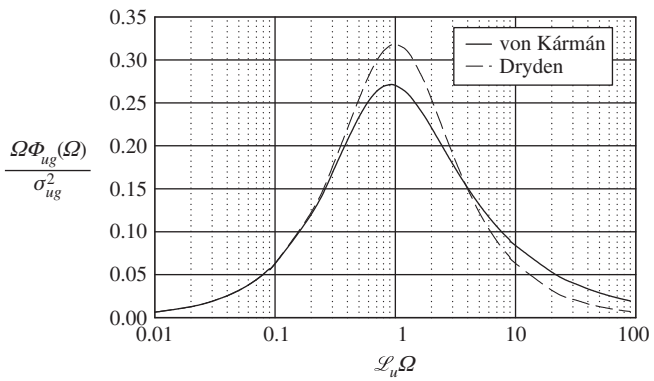

FIGURE 14.2 Comparison of Von Kármán and Dryden power spectra for the axial component of turbulence velocity.

14.5.4 Turbulence scale length

The determination of the appropriate scale, or scale length, of continuous turbulence remains probably one of the most contentious issues in turbulence modelling, and opinions differ among those involved in its application. As aircraft technology has advanced and flight envelopes have expanded, questions have been raised concerning the appropriateness of the scale length requirements set out in

Def-Stan 00-970 and in MIL-F-8587C. Changes have been made from time to time in an attempt to improve their relevance, and it is likely that this process will continue into the future.

Scale length is very much dependent on height above the local terrain, and the definitions for use in the von Kármán power spectra as set out in Def-Stan 00-970 are given in Table 14.8.

The scale length as set out in MIL-F-8785C is similar, but is defined differently as shown in Table 14.9.

It is interesting to compare the turbulence scale length definitions as given in Tables 14.8 and 14.9; the comparisons are plotted in Fig. 14.3. Of particular interest is the comparison of the low-altitude scale length models, which are clearly rather different.

The key to the plots is given in Table 14.10.

Table 14.8 Turbulence Scale Length Def-Stan 00-970

Height h	**Scale Length** $\mathscr{L}$
Above 750 m (2500 ft)	$\mathscr{L}_u = \mathscr{L}_v = \mathscr{L}_w = 750$ m (2500 ft)
Below 750 m (2500 ft)	$\mathscr{L}_u = \mathscr{L}_v = 82.5h^{\frac{1}{3}}$ m $(184h^{\frac{1}{3}}$ ft)
	$\mathscr{L}_w = h$

Table 14.9 Turbulence Scale Length MIL-F-8785C

Height h	**Scale Length** $\mathscr{L}$
Medium to high altitude, above 2000 ft	$\mathscr{L}_u = \mathscr{L}_v = \mathscr{L}_w = 2500$ ft (von Kármán form)
Medium to high altitude, above 2000 ft	$\mathscr{L}_u = \mathscr{L}_v = \mathscr{L}_w = 1750$ ft (Dryden form)
Low altitude $10 < h < 1000$ ft	$\mathscr{L}_u = \mathscr{L}_v = \dfrac{h}{(0.177 + 0.000823h)^{1.2}}$ ft
	$\mathscr{L}_w = h$

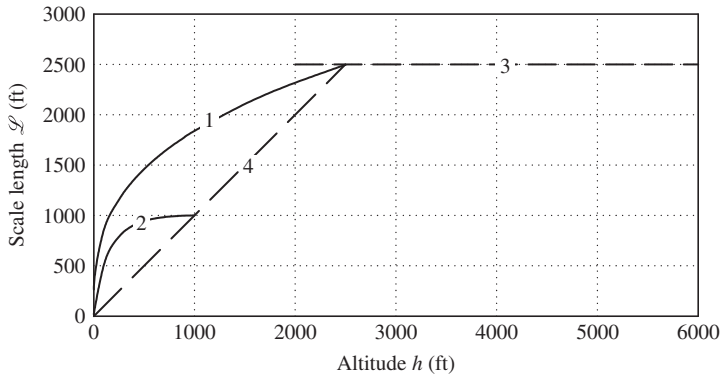

FIGURE 14.3 Comparison of turbulence scale lengths as a function of altitude for Def-Stan 00-970 and MIL-F-8785C.

Table 14.10 Key to Fig. 14.3

Plot	Altitude Range	Def-Stan 00-970	MIL-F-8785C
1	Low altitude to 2500 ft	$\mathscr{L}_u = \mathscr{L}_v$	—
2	Low altitude to 1000 ft	—	$\mathscr{L}_u = \mathscr{L}_v$
3	Medium to high altitude	$\mathscr{L}_u = \mathscr{L}_v = \mathscr{L}_w$ above 2500 ft	$\mathscr{L}_u = \mathscr{L}_v = \mathscr{L}_w$ above 2000 ft
4	Low altitude	$\mathscr{L}_w$ to 2500 ft	$\mathscr{L}_w$ to 1000 ft

It can be seen that the low-altitude scale length defined by MIL-F-8785C applicable to the altitude interval 1000 to 2000 ft is unspecified, although it is not difficult to make a representative estimate from the information available. However, it should be noted that the alternative formulations for defining low altitude scale length are equally acceptable but should be applied in the context of their source document, either Def-Stan 00-970 or MIL-F-8785C.

14.5.5 Turbulence intensity

The reference rms gust and turbulence intensity σ_g in Def-Stan 00-970 is specified as a function of altitude, as shown in Fig. 14.1 and in a similar chart in MIL-F-8785C. The magnitudes of the gust and turbulence velocity component intensities then derive from the reference value.

For the von Kármán model in Def-Stan 00-970, the gust and turbulence component intensities are defined in SI units appropriate to low altitude, below 750 m (2500 ft), as

$$\frac{\sigma_{ug}}{\mathscr{L}_u^{\frac{1}{3}}} = \frac{\sigma_{vg}}{\mathscr{L}_v^{\frac{1}{3}}} = \frac{\sigma_{wg}}{\mathscr{L}_w^{\frac{1}{3}}} = \frac{\sigma_g}{750^{\frac{1}{3}}} \tag{14.45}$$

and at medium to high altitude above 750 m, equation (14.40) simplifies to

$$\sigma_{ug} = \sigma_{vg} = \sigma_{wg} = \sigma_g \tag{14.46}$$

Equation (14.46) is also defined in MIL-F-8785C, in the equivalent American imperial units, for medium to high altitudes above 2000 ft. For low altitude, below 1000 ft, the gust and turbulence component intensities are defined differently:

$$\frac{\sigma_{ug}}{\sigma_{wg}} = \frac{\sigma_{vg}}{\sigma_{wg}} = \frac{1}{(0.177 + 0.000823h)^{0.4}} \tag{14.47}$$

and

$$\sigma_{wg} = 0.1u_{20} \tag{14.48}$$

where u_{20} is the mean wind velocity at 20 ft above the local terrain. Additional information is provided to quantify *light*, *moderate*, and *severe* values for u_{20}, as set out in Table 14.11, and to quantify the probability of exceeding a given reference value.

With reference to the definitions of scale length in Table 14.9, it is easily shown that equation (14.47) may be written alternatively as

$$\frac{\sigma_{ug}}{\mathscr{L}_u^{\frac{1}{3}}} = \frac{\sigma_{vg}}{\mathscr{L}_v^{\frac{1}{3}}} = \frac{\sigma_{wg}}{\mathscr{L}_w^{\frac{1}{3}}} \tag{14.49}$$

Table 14.11 Mean Wind Speed at 20 ft

Intensity	Reference Value u_{20} (knots)
Light	15
Moderate	30
Severe	45

which is identical to equation (14.45). However, it should be remembered that the gust and turbulence scale lengths are defined differently in MIL-F-8785C, as described in Section 14.5.4. This is yet another example which shows that the general approach to mathematical modelling of turbulence is universally accepted but that opinions continue to differ about the way in which scale length should be defined.

Gust and turbulence intensities, expressed in American imperial units, for the Dryden model are, for altitudes below 1750 ft,

$$\frac{\sigma_{ug}^2}{\mathscr{L}_u} = \frac{\sigma_{vg}^2}{\mathscr{L}_v} = \frac{\sigma_{wg}^2}{\mathscr{L}_w} = \frac{\sigma_g^2}{1750} \tag{14.50}$$

and for the intensity of the rotational roll turbulence component it is

$$\sigma_{pg} = \frac{1.9\sigma_{wg}}{(\mathscr{L}_w b)^{\frac{1}{2}}} \tag{14.51}$$

At medium to high altitude above 1750 ft, equation (14.46) applies.

14.6 Discrete gusts

The discrete gust is assumed to be an isolated event which can occur in clear air or can be embedded in a patch of continuous turbulence. When it is embedded in continuous turbulence, the gust shape and its spectral properties are assumed to be related to those of the turbulence. For the purposes of flying qualities evaluations, the gust can take the form of a linear ramp or step function. The essential requirement is that the gust should be defined to excite the aircraft at known resonant frequencies, giving rise to the concept of the *tuned gust*. The preferred gust shapes are based on the "1-cosine" gust, the properties of which can be designed as required to suit the application and which is entirely compatible with the energy distribution of the von Kármán power spectrum.

14.6.1 The "1-cosine" gust

Typical gust shapes are shown in Fig. 14.4. A gust is defined as the ramp-up, or ramp-down, over the gust length distance d. The same shapes and definitions apply to the axial, lateral, and normal gust velocity components u_g, v_g, and w_g, respectively. Fig. 14.4a shows a symmetric gust, and as the aircraft traverses the gust the velocity V_g ramps up to its maximum value V_{gm} over the distance d and then ramps down again over the same distance. The "1-cosine" function defines the shape of

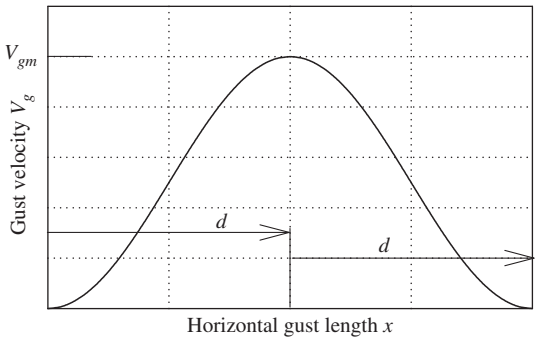

FIGURE 14.4 Typical "1-cosine" gust shapes.

the initial velocity ramp-up to its maximum value and the decay to zero following the peak. The time and frequency properties of the gust are determined by the velocity at which the aircraft traverses it, and d is chosen to excite the aircraft at known resonant frequencies in an attempt to obtain the maximum response for the chosen gust magnitude. The maximum gust velocity V_{gm}, or gust magnitude, is chosen according to the required gust intensity: light, moderate, or severe. The functions describing the gust shape are

$$\text{Ramp-up} \quad V_g = \frac{V_{gm}}{2}\left(1 - \cos\left(\frac{\pi x}{d}\right)\right) \tag{14.52}$$

$$\text{Ramp-down} \quad V_g = \frac{V_{gm}}{2}\left(1 + \cos\left(\frac{\pi x}{d}\right)\right) \tag{14.53}$$

Similarly, alternative shapes can be built up using the "1-cosine" gust function, and a typical example of an asymmetric gust is shown in Fig. 14.4b. In this model, the gust ramps up to a maximum velocity over the distance d_1, holds the maximum velocity over the distance d_2, and finally ramps down over the distance d_3 to a non-zero velocity. Clearly, this approach to gust modelling can be used to create any arbitrary tuned gust shape.

14.6.2 Determination of maximum gust velocity and horizontal length

The determination of maximum gust velocity and horizontal length d is treated rather differently in MIL-F-8785C and Def-Stan 00-970. In both cases the determination of gust length is left to the discretion of the investigator and should be chosen to excite the aircraft at a known resonant frequency. For example, in the present context, where only rigid body motion is a consideration, the gust length might be chosen to excite one of the stability modes. The determination of maximum gust velocity is a function of gust length, altitude, and the reference intensity σ_g, as given by Fig. 14.1, or the equivalent in MIL-F-8785C.

The empirical relationship between gust magnitude and gust length is given in MIL-F-8785C in normalised form, as shown in Fig. 14.5, and is applicable for light and moderate intensity gusts only at all altitudes. Severe gust velocity is quantified as a function of aircraft velocity, altitude, and aircraft operating configuration; values are quoted for a number of critical flight conditions, the maximum value quoted being $V_{gm} = 66$ ft/s, which represents a worst case situation for analytical purposes.

A different empirical relationship between gust magnitude and gust length is given in Def-Stan 00-970. The requirements set out in Def-Stan 00-970 have been normalised to facilitate comparison with MIL-F-8785C and are given in Table 14.12 (SI units apply). Notable observations are

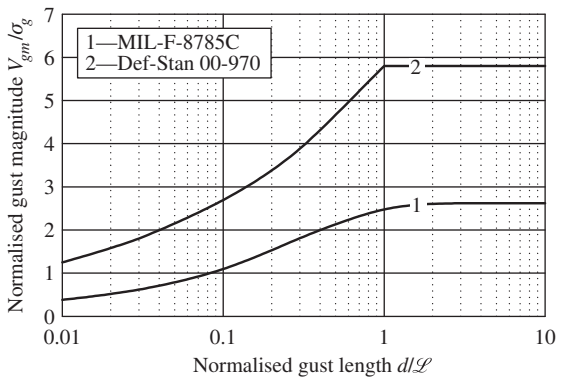

FIGURE 14.5 Normalised gust magnitude and length.

Table 14.12 Normalised Gust Magnitude and Length components as given in Def-Stan 00-970

$d \le \mathscr{L}$	$d \ge \mathscr{L}$
$\frac{u_{gm}}{\sigma_g} = 1.25J\left(\frac{\mathscr{L}_u}{750}\frac{d_x}{\mathscr{L}_u}\right)^{\frac{1}{3}}$	$\frac{u_{gm}}{\sigma_g} = 1.25J\left(\frac{\mathscr{L}_u}{750}\right)^{\frac{1}{3}}$
$\frac{v_{gm}}{\sigma_g} = 1.45J\left(\frac{\mathscr{L}_v}{750}\frac{d_y}{\mathscr{L}_v}\right)^{\frac{1}{3}}$	$\frac{v_{gm}}{\sigma_g} = 1.45J\left(\frac{\mathscr{L}_v}{750}\right)^{\frac{1}{3}}$
$\frac{w_{gm}}{\sigma_g} = 1.45J\left(\frac{\mathscr{L}_w}{750}\frac{d_z}{\mathscr{L}_w}\right)^{\frac{1}{3}}$	$\frac{w_{gm}}{\sigma_g} = 1.45J\left(\frac{\mathscr{L}_w}{750}\right)^{\frac{1}{3}}$

that when the gust length d is smaller than the turbulence scale length $\mathscr{L}$ the gust magnitude varies with gust length; when d is greater than $\mathscr{L}$, the gust magnitude is independent of turbulence scale length.

The scale factor J is set at a provisional value of 4.0, but uncertainty is expressed as to exactly what its value should be. Again, this illustrates the difficulty of quantifying atmospheric disturbances in an appropriate way for flying qualities evaluations. The difference between the requirements in MIL-F-8785C and Def-Stan 00-970 become clear when the normalised component magnitude w_{gm}/σ_g from Table 14.12 is plotted on Fig.4.5. It is interesting that the plots are nominally of the same shape but that Def-Stan 00-970 consistently estimates larger gust velocity magnitude than does MIL-F-8785C; this is found to be the case for all gust velocity components over the altitude range.

14.7 Aircraft response to gusts and turbulence

As stated earlier, most applications of aircraft gust and turbulence response relate to the non-linear, continuous-time simulation environment. In this context it is possible to get much closer to reality, especially in the piloted simulation environment. In comparison, the application of gust and turbulence modelling in the linear rigid body dynamics context is of limited scope. However, such limited evaluations as can be made provide a useful preliminary means for assessing aircraft and flight control system performance in non-steady atmospheric conditions. Consequently, the following material is included for completeness, but it is important to realise that its usefulness is limited by the constraints of linearised rigid body modelling.

14.7.1 Variance, power spectral density, and white noise

The application of Parseval's theorem enables the average power, or *variance* σ^2, of a time-varying random signal $u(t)$ to be determined from either its time domain description or its frequency domain description; thus

$$\sigma_u^2 = \int_{-\infty}^{\infty} u^2(t)\mathrm{d}t = \int_{-\infty}^{\infty} \left|u(f)\right|^2 \mathrm{d}f = \int_{-\infty}^{\infty} \Phi_u(f)\mathrm{d}f \tag{14.54}$$

where f is the *cyclic* frequency (Hz). Since linear systems frequency domain analysis is usually expressed in terms of *angular* frequency ω (rad/s) then, alternatively, it is convenient to write equation (14.54) as

$$\sigma_u^2 = \int_{-\infty}^{\infty} u^2(t)\mathrm{d}t = \frac{1}{2\pi}\int_{-\infty}^{\infty} \left|u(\omega)\right|^2 \mathrm{d}\omega = \frac{1}{2\pi}\int_{-\infty}^{\infty} \Phi_u(\omega)\mathrm{d}\omega \tag{14.55}$$

Now, if the function $u(t)$ is symmetric about $t = 0$ such that $u(-t) = u(t)$, then, equivalently, equation (14.55) may be written as

$$\sigma_u^2 = \frac{1}{\pi}\int_{0}^{\infty} \left|u(\omega)\right|^2 \mathrm{d}\omega = \frac{1}{\pi}\int_{0}^{\infty} \Phi_u(\omega)\mathrm{d}\omega \tag{14.56}$$

In practical applications to real systems, integration over all positive frequencies is standard practice and the "single-sided" expression given by equation (14.56) is in common use.

Thus the PSD of $u(t)$ is given by

$$\Phi_u(\omega) = |u(\omega)|^2 \text{ with units } (\text{m/s})^2/(\text{rad/s}) \text{ or } (\text{ft/s})^2/(\text{rad/s}) \tag{14.57}$$

$$\Phi_u(f) = \left|u(f)\right|^2 \text{ with units } (\text{m/s})^2/\text{Hz} \text{ or } (\text{ft/s})^2/\text{Hz} \tag{14.58}$$

Note that the definitions and units of PSD are emphasized here since it is essential to be precise when dealing with turbulence models if inconsistencies are to be avoided. It is particularly important to note that the definition of variance used in both Def-Stan 00-970 and MIL-F-8785C is derived from equation (14.54) and quoted as

$$\sigma^2 = \int_0^\infty \Phi(\omega)\mathrm{d}\omega$$

in which ω is defined as *angular frequency*. However, this formulation of the definition of variance usually assumes a *cyclic frequency* dependency (compare with equation (14.54)), and the inconsistency can be confusing. On the other hand, the computational algorithm used by both MATLAB and Program CC to calculate variance implements equation (14.56) directly. Clearly, this implies an *angular frequency* dependency, which is entirely consistent with the mathematics of linear systems. Since MATLAB and Program CC share the same mathematical origins, many of their computational algorithms are the same; in the present context this applies to *variance*, *covariance*, and *Lyapunov equation* calculations. Consequently, particular care is required when using MATLAB, Program CC, and similar computational tools for atmospheric variance calculations to ensure that the factor $1/\pi$ is correctly allocated. It is considered good practice to check that rms values calculated in the time and frequency domains are consistent.

It is useful now to consider the *rms intensity*, or *standard deviation* σ_u of the random signal $u(t)$ in a practical context, where typically

$$\begin{aligned} u(t) &= 0 \quad \text{for} \quad t < 0 \\ u(t) &\neq 0 \quad \text{for} \quad 0 \leq t \leq T \end{aligned} \tag{14.59}$$

For such a series expression, $u(-t) = u(t)$ can be redefined to allow use of the single-sided integral expression given by equation (14.56).

Assume that n samples of $u(t)$ are recorded in the interval $0 \leq t \leq T$ and that $u(t)$ is a *zero mean value* signal; then

$$\overline{u}(t) = \frac{1}{n}\sum_{i=1}^{n} u_i(t) = 0 \tag{14.60}$$

and the rms intensity of $u(t)$ is defined by

$$\sigma_u = \sqrt{\frac{1}{n}\sum_{i=1}^{n} u_i^2(t)} \tag{14.61}$$

Alternatively, rms intensity may be expressed as a function of power spectral density. When the frequency spectrum is expressed in terms of cyclic frequency f, equation (14.54) applies:

$$\sigma_u = \sqrt{\int_0^\infty \left|u(f)\right|^2 \mathrm{d}f} = \sqrt{\int_0^\infty \Phi_u(f)\mathrm{d}f} \tag{14.62}$$

Or, in terms of angular frequency ω, equation (14.56) applies:

$$\sigma_u = \sqrt{\frac{1}{\pi}\int_0^\infty |u(\omega)|^2 \mathrm{d}\omega} = \sqrt{\frac{1}{\pi}\int_0^\infty \Phi_u(\omega)\mathrm{d}\omega} \tag{14.63}$$

A *white noise* signal is an artefact of the engineer devised for the convenience of representing naturally occurring random phenomena in engineering applications. In the present context, synthetic turbulence is "manufactured" by filtering a white noise signal such that its output power spectrum matches "real" turbulence as far as that is possible. A white noise signal $N(t)$ is defined as having zero mean value and uniform power distribution over the frequency spectrum $-\infty<f<\infty$ Hz, or $-\infty<\omega<\infty$ rad/s. It follows that "unit" white noise has the following statistical properties which are independent of frequency:

$$\begin{array}{ll} \text{Power spectral density} & \Phi_N(f) = \Phi_N(\omega) = 1.0 \\ \text{Variance} & \sigma_N^2 = 1.0 \\ \text{Standard deviation, or rms intensity} & \sigma_N = 1.0 \\ \text{Mean} & \overline{N}(t) = 0 \end{array} \tag{14.64}$$

The action of filtering white noise produces bandwidth limited white noise, which also has zero mean and a uniform power distribution over the reduced frequency spectrum. Thus, for "unit" white noise input, the output variance and rms intensity also have unit values.

14.7.2 Spatial and temporal equivalence

Gusts and turbulence are characterised by their magnitude and the size of the horizontal area, or patch, over which they occur. Their spectral properties are quantified in terms of spatial frequency Ω, or radians per unit distance. On the other hand, aircraft response to gusts and turbulence is quantified in terms of temporal frequency ω and the temporal characteristics of the disturbance are quantified by the time taken for the aircraft to traverse the gust or patch of turbulence. Assuming frozen turbulence, the time taken for an aircraft travelling at velocity V_0 to traverse a gust or patch of turbulence of size d is given by

$$t = \frac{d}{V_0} \tag{14.65}$$

Consequently, the equivalence between spatial and temporal frequency is given by

$$\omega = V_0\Omega \tag{14.66}$$

and it follows that the equivalence between temporal and spatial turbulence power spectra is given by

$$\Phi_i(\omega) = \frac{1}{V_0}\Phi_i(\Omega) \quad i = u_g,\ v_g,\ w_g \tag{14.67}$$

The rise time t of a discrete gust is given by equation (14.65), and it follows that the period associated with the gust is given by

$$T_g = \frac{2\pi}{\omega} = \frac{2d}{V_0} \tag{14.68}$$

Clearly, the temporal frequency spectrum of turbulence is entirely dependent on the velocity at which the aircraft traverses the patch, and the excitation frequency of a discrete gust is similarly determined by the velocity at which the aircraft traverses the gust ramp. Equation (14.68) provides

the means for determining the suitable gust length d necessary to excite the aircraft at a particular frequency, corresponding, for example, with one of the rigid body stability modes.

14.7.3 Synthetic turbulence

It is usual to synthesize artificial turbulence models by passing white noise through a filter with a transfer function designed to produce an output turbulence velocity component having the correct power spectrum. Gage (2003) discusses at length the difficulties of developing a unified approach for creating MATLAB models and procedures for sythesizing atmospheric turbulence from the various models specified. Given particular attention is the especially difficult problem of modelling the von Kármán power spectra. Thus the problem of generating artificial turbulence reduces to that of designing a family of white noise filters. The process is represented in Fig. 14.6, where $i = u_g, v_g, w_g$.

The relationship between the input and output power spectra is given by

$$\Phi_i(\omega) = \left|G_i(s)\right|^2_{s=j\omega}\Phi_N(\omega) = \left|G_i(s)\right|^2_{s=j\omega} \tag{14.69}$$

since the PSD of white noise is defined as $\Phi_N(\omega) = 1.0$ (σ^2/rad/s).

To illustrate the filter design process, consider synthesizing the axial turbulence velocity component u_g using the Dryden spectral form, for which the power spectrum is given by equation (14.36). With reference to equations (14.66) and (14.67), the temporal PSD may be written as

$$\Phi_{ug}(\omega) = \sigma^2_{ug}\frac{2\mathscr{L}_u}{\pi V_0}\frac{1}{\left(1+\left(\dfrac{\mathscr{L}_u}{V_0}\omega\right)^2\right)} \tag{14.70}$$

With reference to equation (14.69) and to the form of equation (14.70), it is evident that a suitable transfer function $G_i(s)$ is given by a simple low-pass filter having the general form

$$G_{ug}(s) = \frac{K_{ug}}{(1+sT_{ug})} \tag{14.71}$$

Whence equation (14.69) may be written as

$$\begin{aligned}\Phi_{ug}(\omega) &= \sigma^2_{ug}\frac{2\mathscr{L}_u}{\pi V_0}\frac{1}{\left(1+\left(\dfrac{\mathscr{L}_u}{V_0}\omega\right)^2\right)} = \left|G_{ug}(s)\right|^2_{s=j\omega}\\ &= G_{ug}(j\omega)G_{ug}(-j\omega)\\ &= \frac{K^2_{ug}}{(1+j\omega T_{ug})(1-j\omega T_{ug})} = \frac{K^2_{ug}}{(1+\omega^2T^2_{ug})}\end{aligned} \tag{14.72}$$

FIGURE 14.6 Turbulence modelling process.

Equating coefficients in equation (14.72), the gain and time constant for the filter are defined:

$$\begin{aligned} K_{ug} &= \sigma_{ug}\sqrt{\frac{2\mathscr{L}_u}{\pi V_0}} = \sigma_{ug}\sqrt{\frac{2T_{ug}}{\pi}} \\ T_{ug} &= \frac{\mathscr{L}_u}{V_0} \end{aligned} \tag{14.73}$$

A more complex illustration is provided by the design of the filter to produce the normal component of turbulence velocity w_g, again using the Dryden form. From equation (14.38) the temporal PSD may be written as

$$\Phi_{wg}(\omega) = \sigma_{wg}^2 \frac{\mathscr{L}_w}{\pi V_0} \frac{\left(1 + 3\left(\frac{\mathscr{L}_w}{V_0}\omega\right)^2\right)}{\left(1 + \left(\frac{\mathscr{L}_w}{V_0}\omega\right)^2\right)^2} \tag{14.74}$$

Equation (14.74) suggests a filter having the following general form:

$$G_{wg}(s) = \frac{K_{wg}(1 + sT_1)}{(1 + sT_2)^2} \tag{14.75}$$

Applying equation (14.69) and substituting equations (14.74) and (14.75), it follows that

$$\Phi_{wg}(\omega) = \sigma_{wg}^2 \frac{\mathscr{L}_w}{\pi V_0} \frac{\left(1 + 3\left(\frac{\mathscr{L}_w}{V_0}\omega\right)^2\right)}{\left(1 + \left(\frac{\mathscr{L}_w}{V_0}\omega\right)^2\right)^2} = \frac{K_{wg}^2(1 + (\omega T_1)^2)}{(1 + (\omega T_2)^2)^2} \tag{14.76}$$

Again, equating coefficients in equation (14.76), the filter gain and time constants are easily identified:

$$\begin{aligned} K_{wg} &= \sigma_{wg}\sqrt{\frac{\mathscr{L}_w}{\pi V_0}} = \sigma_{wg}\sqrt{\frac{T_{wg}}{\pi}} \\ T_1 &= \sqrt{3}T_{wg} = \sqrt{3}\frac{\mathscr{L}_w}{V_0} \\ T_2 &= T_{wg} = \frac{\mathscr{L}_w}{V_0} \end{aligned} \tag{14.77}$$

Whence transfer function (14.75) may be written as

$$G_{wg}(s) = \frac{K_{wg}\left(1 + \sqrt{3}T_{wg}s\right)}{(1 + T_{wg}s)^2} \tag{14.78}$$

Similarly, the lateral component of turbulence velocity v_g is derived from the Dryden temporal PSD form of equation (14.37) to give the filter

$$G_{vg}(s) = \frac{K_{vg}\left(1 + \sqrt{3}T_{vg}s\right)}{(1 + T_{vg}s)^2} \tag{14.79}$$

where

$$K_{vg} = \sigma_{vg}\sqrt{\frac{\mathscr{L}_v}{\pi V_0}}$$
$$T_{vg} = \frac{\mathscr{L}_v}{V_0} \tag{14.80}$$

14.7.4 Aircraft response to gusts

In the context of linear rigid body modelling, aircraft gust response can be analysed by creating a gust model and using it as the input to the aircraft equations of motion, as described in Section 14.4. Now the spatial description of the tuned gust is given by equation (14.52); since aircraft response is a time-dependent property, it is first necessary to define the gust shape in terms of the desired temporal excitation frequency ω_g, where, for example, ω_g would be chosen (tuned) to excite the aircraft at a known aircraft mode frequency.

With reference to equation (14.52), the distance variable x is related to the time variable t by the aircraft velocity V_0 through

$$x = V_0 t \tag{14.81}$$

and from equation (14.68) the gust length d is defined in terms of temporal frequency ω_g as

$$d = \frac{\pi V_0}{\omega_g} \tag{14.82}$$

Whence it is easily shown that the temporal equivalent of equation (14.52) is

$$V_g(t) = \frac{V_{gm}(t)}{2}(1 - \cos\omega_g t) \tag{14.83}$$

and the equivalent of equation (14.53) may be similarly stated.

Having defined the gust length d, the turbulence scale length $\mathscr{L}$ is determined for the flight condition as described in Section 14.5.4. To complete the gust model the maximum gust velocity V_{gm} may then be determined as described in Section 14.6.2.

To create a disturbance input for the aircraft equations of motion, a gust input vector $\mathbf{u}_g(t)$ is assembled using equation (14.83) to build a time sequence of gust shapes to suit the investigation at hand.

EXAMPLE 14.2

In the interests of simplicity and continuity, this example builds on the model of the Douglas DC-8 developed in Example 14.1, the main task here being to create a suitable gust disturbance model and then to assess the aircraft response to the gust.

The chosen requirement is to create a normal gust w_g of *moderate* intensity such that the ramp-up to maximum velocity is tuned to the longitudinal short-period pitching oscillation. The maximum velocity is then held constant for a few seconds, and the final ramp-down is tuned to the phugoid mode. The flying qualities requirements in MIL-F-8785C are applied, and the Dryden turbulence model is assumed.

The essential data from Example 14.1 are

Altitude $h = 15{,}000$ ft
Velocity $V_0 = 468.2$ ft/s
Phugoid damping ratio $\zeta_p = 0.031$
Phugoid natural frequency $\omega_p = 0.088$ rad/s
Short-period damping ratio $\zeta_s = 0.435$
Short-period natural frequency $\omega_s = 2.4$ rad/s

From MIL-F-8785C the scale length and gust intensity are determined

Dryden scale length at 15,000 ft (see Table 14.9): $\mathscr{L}_w = 1750$ ft
Moderate rms gust intensity at 15,000 ft: $\sigma_g = 9$ ft/s

For the gust ramp-up tuned to the short-period mode frequency ω_s, the gust length given by equation (14.68) is

$$d_s = \frac{\pi V_0}{\omega_s} = 612.87 \text{ ft} \tag{14.84}$$

and the time taken to traverse this distance is $t = d_s/V_0 = 1.3$ s. Now, since $d_s/\mathscr{L}_w = 0.35$, from the appropriate plot in Fig. 14.5,

$$V_{gm} = 1.9\sigma_g = 17.1 \text{ ft/s}$$

Substituting ω_s and V_{gm} into equation (14.83) gives the initial gust ramp-up tuned to the short-period mode:

$$w_{g1}(t) = \frac{V_{gm}(t)}{2}(1 - \cos\omega_s t) = 8.55(1 - \cos 2.4t) \quad \text{for } t = 0 \text{ to } 1.3 \text{ s} \tag{14.85}$$

For the constant section of the gust following the ramp-up, let the time description be

$$w_{g2} = 1.71 \quad \text{for } t = 1.4 \text{ to } 3.9 \text{ s} \tag{14.86}$$

For the gust ramp-down, following the constant section, tuned to the phugoid mode frequency ω_p, the gust length given by equation (14.68) is

$$d_p = \frac{\pi V_0}{\omega_p} = 16714.7 \text{ ft} \tag{14.87}$$

and the time taken to traverse this distance is $t = d_p/V_0 = 35.7$ s. Again, since $d_p/\mathscr{L}_w = 9.55$, from the appropriate plot on Fig. 14.5,

$$V_{gm} = 2.6\sigma_g = 23.4 \text{ ft/s}$$

Thus, for a gust correctly tuned to the phugoid mode, the maximum gust velocity corresponding to a *moderate* gust intensity is 23.4 ft/s. However, purely for the convenience of this illustration, it is required that the gust sequence conclude at $w_g = 0$; thus the maximum value V_{gm} used for the ramp-down remains at 17.1 ft/s, as for the ramp-up. This implies that, although the gust ramp-down is correctly tuned to the phugoid frequency, its magnitude corresponds with an intensity which is less than moderate. Accordingly, the time description of the ramp-down is

$$w_{g3}(t) = \frac{V_{gm}(t)}{2}(1 + \cos\omega_p t) = 8.55(1 + \cos 2.4t) \quad \text{for } t = 4 \text{ to } 39.7 \text{ s} \tag{14.88}$$

The gust vector comprising the time sequence of gusts was assembled by evaluating equations (14.85), (14.86), and (14.88) over a period of 40 s at 0.1-s time intervals to give

$$w_g = (w_{g1};\ w_{g2};\ w_{g3}) \tag{14.89}$$

The gust sequence computed according to equation (14.89) is shown in Fig. 14.7, where the indicators 1, 2, and 3 denote the gust contributions w_{g1}, w_{g2}, and w_{g3}, respectively.

To evaluate the DC-8 response to the shaped gust shown in Fig. 14.7, the gust vector w_g given by equation (14.89) is used as the input vector to the aircraft equations of motion (14.30), and then subject to the linear simulation computation in MATLAB or Program CC. When the simulation is run for a total of 50 s, the output response variables obtained are shown in Fig. 14.8. It is quite clear that the gust sequence excites both the short-period and phugoid modes, as intended, and that the settling times are consistent with the mode damping ratios.

The short-term response, associated with the short-period mode dynamics, shows a peak in normal load factor n_z of $-0.2\ g$ at about 1 s, and a peak in pitch attitude θ of approximately 1.7 deg at around 2.5 s. Since the longer-term response to the gust sequence is governed by the phugoid dynamics, it is not surprising to see that the peak in normal load factor n_z at around 45 s is very small whereas the peaks in the velocity u and pitch attitude θ perturbations are more evident. The peak in velocity u is approximately 15 ft/s and occurs at about 46 s, and the peak in pitch attitude θ is approximately 2.5 deg and occurs at about 34 s.

14.7.5 Aircraft response to turbulence

For practical reasons, the analytical investigation of aircraft response to atmospheric turbulence is limited when using linear rigid body modelling methods. Typical investigations are confined to the

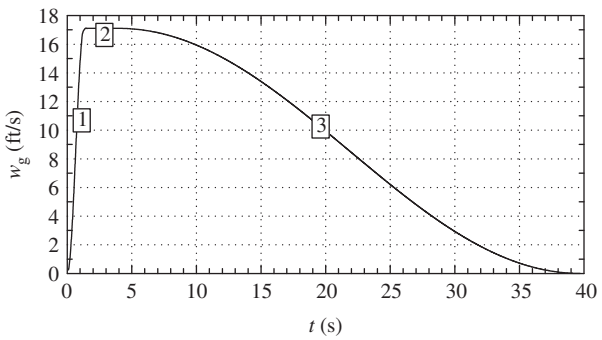

FIGURE 14.7 Tuned w_g gust input.

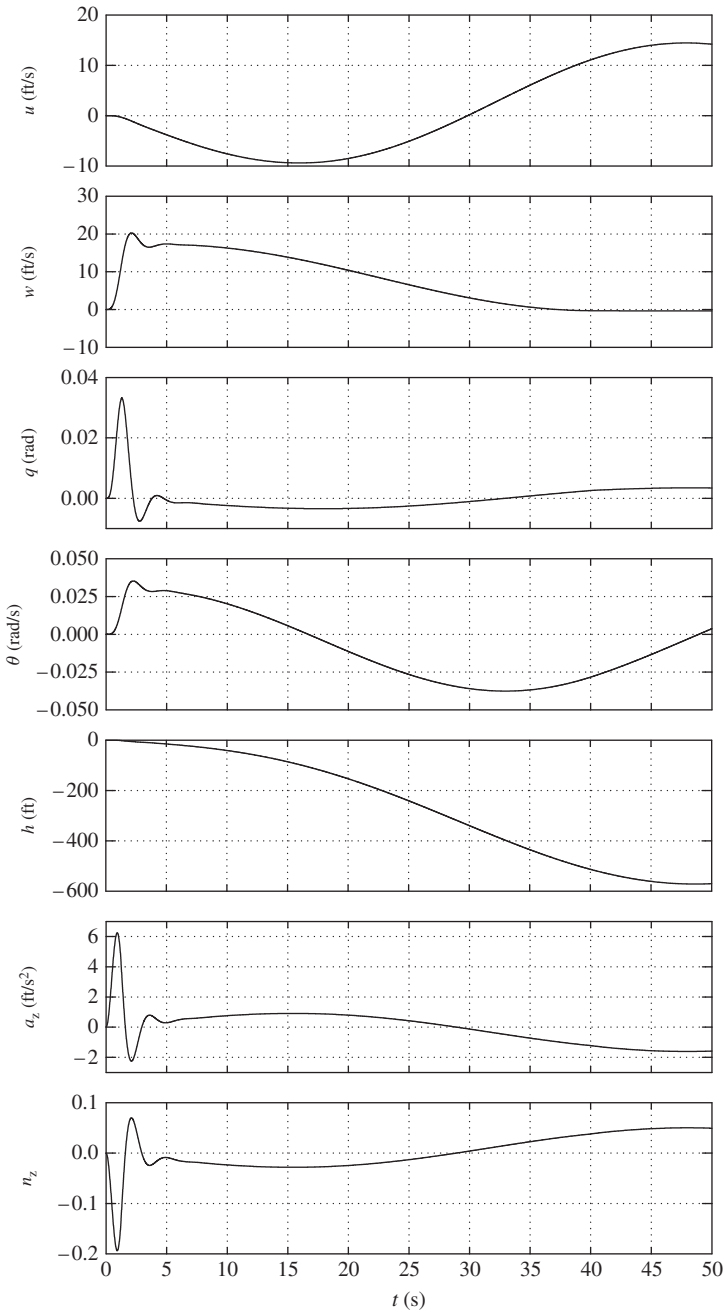

FIGURE 14.8 DC-8 response to a tuned w_g gust of moderate intensity.

evaluation of frequency response properties. More searching investigations would properly be undertaken using non-linear simulation methods as explained previously.

The system model for analytical investigation is shown in Fig. 14.9, where $G_f(t)$ denotes the noise filtering required to generate the turbulence velocity components from a white noise signal input $N(t)$, and $G_A(t)$ denotes the aircraft equations of motion describing the output response $y(t)$ to the turbulence inputs. For analysis, then, the problem simplifies to solution of equation (14.90):

$$y(t) = G_f(t)G_A(t)N(t) \tag{14.90}$$

With reference to equations (14.22), the aircraft state equation may be written as

$$\dot{\mathbf{x}} = \mathbf{A}\mathbf{x} + \mathbf{E}\mathbf{u}_g \tag{14.91}$$

where here the state matrix $\mathbf{A}$ represents the aircraft with or without stability augmentation as appropriate. Similarly, the state equation representing the noise filter may be realised as

$$\dot{\mathbf{x}}_f = \mathbf{A}_f\mathbf{x}_f + \mathbf{B}_f N \tag{14.92}$$

Thus the state equation for the system shown in Fig. 14.9 may be assembled by augmenting the aircraft state equation (14.91) with the filter state equation (14.92):

$$\left[\begin{array}{c}\dot{\mathbf{x}}\\ \hline \dot{\mathbf{x}}_f\end{array}\right] = \left[\begin{array}{c|c}\mathbf{A} & 0\\ \hline 0 & \mathbf{A}_f\end{array}\right]\left[\begin{array}{c}\mathbf{x}\\ \hline \mathbf{x}_f\end{array}\right] + \left[\begin{array}{c}\mathbf{E}\\ \hline 0\end{array}\right]\mathbf{u}_g + \left[\begin{array}{c}0\\ \hline \mathbf{B}_f\end{array}\right]N \tag{14.93}$$

Consider, for example, the case when the aircraft response to an axial velocity turbulence component is required. From equations (14.14), the longitudinal state equation for the aircraft for the single input u_g, referred to wind axes, may be written in concise form as

$$\begin{bmatrix}\dot{u}\\ \dot{w}\\ \dot{q}\\ \dot{\theta}\end{bmatrix} = \begin{bmatrix}x_u & x_w & x_q & -g\\ z_u & z_w & z_q & 0\\ m_u & m_w & m_q & 0\\ 0 & 0 & 1 & 0\end{bmatrix}\begin{bmatrix}u\\ w\\ q\\ \theta\end{bmatrix} + \begin{bmatrix}-x_u\\ -z_u\\ -m_u\\ 0\end{bmatrix}u_g \tag{14.94}$$

which is the single-input realisation of equation (14.91). Using the Dryden gust filter transfer function as given by equation (14.71), this may be written as

$$\frac{u_g(s)}{N(s)} = \frac{K_{ug}}{(1 + sT_{ug})} \tag{14.95}$$

Alternatively, equation (14.95) may be written as

$$u_g(s) + su_g(s)T_{ug} = K_{ug}N(s) \tag{14.96}$$

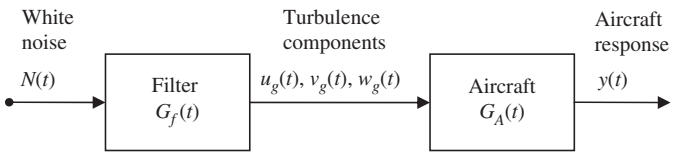

FIGURE 14.9 Analytical system model.

The inverse Laplace transform of equation (14.96) is

$$\dot{u}_g(t)T_{ug} = -u_g(t) + K_{ug}N(t)$$

or

$$\dot{u}_g = -\frac{1}{T_{ug}}u_g + \frac{K_{ug}}{T_{ug}}N \tag{14.97}$$

Note that, in taking the inverse Laplace transform of equation (14.96), zero initial conditions are assumed, which is consistent with the linear systems assumption that aircraft motion is referred to trimmed equilibrium. Equation (14.97) is the state equation for the u_g filter and is the realisation of equation (14.92). Thus equations (14.94) and (14.97) may be substituted into equation (14.93) to give the augmented aircraft state equation describing aircraft response to axial velocity turbulence:

$$\begin{bmatrix} \dot{u} \\ \dot{w} \\ \dot{q} \\ \dot{\theta} \\ \dot{u}_g \end{bmatrix} = \begin{bmatrix} x_u & x_w & x_q & -g & -x_u \\ z_u & z_w & z_q & 0 & -z_u \\ m_u & m_w & m_q & 0 & -m_u \\ 0 & 0 & 1 & 0 & 0 \\ 0 & 0 & 0 & 0 & -\dfrac{1}{T_{ug}} \end{bmatrix} \begin{bmatrix} u \\ w \\ q \\ \theta \\ u_g \end{bmatrix} + \begin{bmatrix} 0 \\ 0 \\ 0 \\ 0 \\ \dfrac{K_{ug}}{T_{ug}} \end{bmatrix} N$$

or, substituting for K_{ug} from equations (14.73),

$$\begin{bmatrix} \dot{u} \\ \dot{w} \\ \dot{q} \\ \dot{\theta} \\ \dot{u}_g \end{bmatrix} = \begin{bmatrix} x_u & x_w & x_q & -g & -x_u \\ z_u & z_w & z_q & 0 & -z_u \\ m_u & m_w & m_q & 0 & -m_u \\ 0 & 0 & 1 & 0 & 0 \\ 0 & 0 & 0 & 0 & -\dfrac{1}{T_{ug}} \end{bmatrix} \begin{bmatrix} u \\ w \\ q \\ \theta \\ u_g \end{bmatrix} + \begin{bmatrix} 0 \\ 0 \\ 0 \\ 0 \\ \sigma_{ug}\sqrt{\dfrac{2}{\pi T_{ug}}} \end{bmatrix} N \tag{14.98}$$

Realising the state descriptions of the Dryden w_g and v_g turbulence filter transfer functions is a little more difficult because they are both of second order. The process is illustrated for the normal component of turbulence w_g, for which the filter transfer function is given by equation (14.78):

$$\frac{w_g(s)}{N(s)} = \frac{K_{wg}\left(1+\sqrt{3}T_{wg}s\right)}{\left(1+T_{wg}s\right)^2} = \frac{K_{wg}\left(1+\sqrt{3}T_{wg}s\right)}{\left(1+2T_{wg}s+T_{wg}^2s^2\right)} \tag{14.99}$$

As before, multiplying out equation (14.99) and taking the inverse Laplace transform gives

$$w_g + 2T_{wg}\dot{w}_g + T_{wg}^2\ddot{w}_g = K_{wg}N + K_{wg}\sqrt{3}T_{wg}\dot{N}$$

or

$$\ddot{w}_g + \frac{2}{T_{wg}}\dot{w}_g + \frac{1}{T_{wg}^2}w_g = \frac{K_{wg}}{T_{wg}^2}N + \frac{\sqrt{3}K_{wg}}{T_{wg}}\dot{N} \tag{14.100}$$

Define a dummy variable v such that

$$v = \dot{w}_g - \frac{\sqrt{3}K_{wg}}{T_{wg}}N \quad \text{or} \quad \dot{w}_g = v + \frac{\sqrt{3}K_{wg}}{T_{wg}}N \tag{14.101}$$

Then

$$\dot{v} = \ddot{w}_g - \frac{\sqrt{3}K_{wg}}{T_{wg}}\dot{N} \tag{14.102}$$

Substituting equations (14.101) and (14.102) into equation (14.100) and rearranging gives

$$\dot{v} + \frac{2}{T_{wg}}v + \frac{1}{T_{wg}^2}w_g = \frac{K_{wg}}{T_{wg}^2}\left(1 - 2\sqrt{3}\right)N \tag{14.103}$$

Now the second-order filter state equation (14.92) may be assembled from equations (14.101) and (14.103):

$$\begin{bmatrix} \dot{w}_g \\ \dot{v} \end{bmatrix} = \begin{bmatrix} 0 & 1 \\ -\dfrac{1}{T_{wg}^2} & -\dfrac{2}{T_{wg}} \end{bmatrix} \begin{bmatrix} w_g \\ v \end{bmatrix} + \begin{bmatrix} \dfrac{\sqrt{3}K_{wg}}{T_{wg}} \\ \dfrac{K_{wg}}{T_{wg}^2}\left(1 - 2\sqrt{3}\right) \end{bmatrix} N$$

or, with reference to equations (14.77),

$$\begin{bmatrix} \dot{w}_g \\ \dot{v} \end{bmatrix} = \begin{bmatrix} 0 & 1 \\ -\dfrac{1}{T_{wg}^2} & -\dfrac{2}{T_{wg}} \end{bmatrix} \begin{bmatrix} w_g \\ v \end{bmatrix} + \begin{bmatrix} \sigma_{wg}\sqrt{\dfrac{3}{\pi T_{wg}}} \\ \sigma_{wg}\sqrt{\dfrac{1}{\pi T_{wg}^3}}\left(1 - 2\sqrt{3}\right) \end{bmatrix} N \tag{14.104}$$

Thus, when the aircraft response to the normal velocity turbulence component is required, the concise longitudinal aircraft equations of motion (14.14) may be referred to wind axes, arranged for the single input w_g, and augmented to include the filter state equation (14.104):

$$\begin{bmatrix} \dot{u} \\ \dot{w} \\ \dot{q} \\ \dot{\theta} \\ \dot{w}_g \\ \dot{v} \end{bmatrix} = \begin{bmatrix} x_u & x_w & x_q & -g & -x_w & 0 \\ z_u & z_w & z_q & 0 & -z_w & 0 \\ m_u & m_w & m_q & 0 & -m_w & 0 \\ 0 & 0 & 1 & 0 & 0 & 0 \\ 0 & 0 & 0 & 0 & 0 & 1 \\ 0 & 0 & 0 & 0 & -\dfrac{1}{T_{wg}^2} & -\dfrac{2}{T_{wg}} \end{bmatrix} \begin{bmatrix} u \\ w \\ q \\ \theta \\ w_g \\ v \end{bmatrix} + \begin{bmatrix} 0 \\ 0 \\ 0 \\ 0 \\ \sigma_{wg}\sqrt{\dfrac{3}{\pi T_{wg}}} \\ \sigma_{wg}\sqrt{\dfrac{1}{\pi T_{wg}^3}}\left(1 - 2\sqrt{3}\right) \end{bmatrix} N \tag{14.105}$$

It is interesting that, in both equations (14.98) and (14.105), the terms in the input vector are multiplied by the gust intensity σ_{ug} and σ_{wg}, respectively. Since the white noise input has an rms intensity of $\sigma_N = 1.0$, the rms magnitude of the filter output response is simply scaled by σ_{ug} or σ_{wg}, respectively.

The incorporation of gust filters for the lateral velocity component v_g and the rotational gust velocity components, p_g, q_g, and r_g into the aircraft equations of motion follows a similar mathematical procedure.

EXAMPLE 14.3

To illustrate the computation of longitudinal aircraft response to normal turbulence velocity w_g, derivative and other data for the Lockheed F-104A Starfighter corresponding to an approach flight condition were obtained from Heffley and Jewell (1972). Since the derivative data are referred to body axes, they were converted to a wind axes reference using the relationships given in Appendix 9, Tables A9.1 and A9.3. The data as given apply to sea level conditions, but it was decided to evaluate the turbulence response at $h = 500$ ft and at the given approach velocity $V_0 = 287$ ft/s, it being assumed that the error due to altitude difference would be small. The longitudinal equations of motion (14.13), including the turbulence input terms, apply:

$$\dot{\mathbf{x}} = \mathbf{A}\mathbf{x} + \mathbf{B}\mathbf{u} + \mathbf{E}\mathbf{u}_g$$

Thus, in terms of concise derivative data and including only the single turbulence input variable, the longitudinal state equation describing the unaugmented aircraft is given by

$$\begin{bmatrix} \dot{u} \\ \dot{w} \\ \dot{q} \\ \dot{\theta} \end{bmatrix} = \begin{bmatrix} -0.08078 & 0.04174 & 0 & -32.2 \\ -0.22536 & -0.56292 & 287 & 0 \\ 4.2872e-5 & -7.155e-3 & -0.40416 & 0 \\ 0 & 0 & 1 & 0 \end{bmatrix} \begin{bmatrix} u \\ w \\ q \\ \theta \end{bmatrix} + \begin{bmatrix} -0.10663 \\ -29.724 \\ -4.781 \\ 0 \end{bmatrix} \delta_s + \begin{bmatrix} -0.04174 \\ 0.56292 \\ 7.1550e-3 \\ 0 \end{bmatrix} w_g \tag{14.106}$$

It must be remembered that American imperial units apply throughout. To evaluate the stability and control properties of the basic airframe, the turbulence input is set at $w_g = 0$ and the transfer functions describing response to control are obtained by solving equation (14.106) in the usual way to give

$$\begin{aligned} \frac{u(s)}{\delta_s(s)} &= \frac{-0.1066(s+0.8184)(s-24.99)(s+36.6)}{(s^2+0.073\,s+0.0232)(s^2+0.801\,s+2.274)} \ \frac{\text{ft/s}}{\text{rad}} \\ \frac{w(s)}{\delta_s(s)} &= \frac{-29.72(s^2+0.0802\,s+0.0251)(s+46.57)}{(s^2+0.073\,s+0.0232)(s^2+0.801\,s+2.274)} \ \frac{\text{ft/s}}{\text{rad}} \\ \frac{q(s)}{\delta_s(s)} &= \frac{-4.799\,s(s+0.1036)(s+0.4937)}{(s^2+0.073\,s+0.0232)(s^2+0.801\,s+2.274)} \ 1/\text{s} \\ \frac{\theta(s)}{\delta_s(s)} &= \frac{-4.799(s+0.1036)(s+0.4937)}{(s^2+0.073\,s+0.0232)(s^2+0.801\,s+2.274)} \end{aligned} \tag{14.107}$$

Inspection of the characteristic polynomial, the common denominator of transfer functions (14.107), reveals the basic airframe stability properties:

Phugoid mode: damping ratio $\zeta_p = 0.24$; frequency $\omega_p = 0.15$ rad/s
Short-period pitching mode: Damping ratio $\zeta_s = 0.27$; frequency $\omega_s = 1.51$ rad/s

The stability and control properties of the basic airframe are quite typical of a combat aircraft of the period and show a stable airframe with an unacceptably low value of pitch damping. The aircraft is fitted with a pitch autostabilisation system, but no information about the system is provided in the reference. Thus, before proceeding with the investigation of turbulence response, it is first necessary to augment the longitudinal stability to an acceptable level by raising the pitch damping. For the purpose of this example, pitch rate feedback to elevator was chosen to raise the pitch damping to approximately $\zeta_s = 0.7$. With the aid of a root locus plot using the transfer function $q(s)/\delta_s(s)$ from transfer functions (14.107), a suitable feedback gain was found to be $K_q = -0.35$ rad/rad/s. Thus, with reference to equation (14.19), the feedback gain matrix is

$$\mathbf{K} = \begin{bmatrix} K_u & K_w & K_q & K_\theta \end{bmatrix} = \begin{bmatrix} 0 & 0 & -0.35 & 0 \end{bmatrix} \tag{14.108}$$

With the pitch rate feedback loop closed, the aircraft equations of motion (14.106) become

$$\dot{\mathbf{x}} = [\mathbf{A} - \mathbf{BK}]\mathbf{x} + \mathbf{Bv} + \mathbf{Eu}_g$$

where now the control input vector $\mathbf{v}$ becomes elevator demand, denoted δ_d. The closed-loop state equation for the aircraft becomes

$$\begin{bmatrix} \dot{u} \\ \dot{w} \\ \dot{q} \\ \dot{\theta} \end{bmatrix} = \begin{bmatrix} -0.08078 & 0.04174 & -0.03732 & -32.2 \\ -0.22536 & -0.56292 & 276.5966 & 0 \\ 4.2872e-5 & -7.155e-3 & -2.0775 & 0 \\ 0 & 0 & 1 & 0 \end{bmatrix} \begin{bmatrix} u \\ w \\ q \\ \theta \end{bmatrix} + \begin{bmatrix} -0.10663 \\ -29.724 \\ -4.781 \\ 0 \end{bmatrix} \delta_d + \begin{bmatrix} -0.04174 \\ 0.56292 \\ 7.1550e-3 \\ 0 \end{bmatrix} w_g \tag{14.109}$$

The closed-loop stability properties of the aircraft may be confirmed on inspection of the characteristic polynomial obtained in the solution of equations (14.109):

$$\Delta(s) = (s^2 + 0.07297\, s + .01667)(s^2 + 11.585\, s + 3.161) = 0 \tag{14.110}$$

and

Phugoid mode: damping ratio $\zeta_p = 0.28$; frequency $\omega_p = 0.13$ rad/s
Short-period pitching mode: damping ratio $\zeta_s = 0.75$; frequency $\omega_s = 1.78$ rad/s

For turbulence response assessment, the equations of motion are required in the formulation of equations (14.22), and this may be achieved by assuming controls-fixed, $\delta_d = 0$, by augmenting equation (14.109) to include the additional height variable h and by assembling the output equation to include both normal acceleration a_z and normal load factor n_z referred to the cg.

The mathematical steps required to complete this development are illustrated in Example 14.1. Accordingly, the state model may be written as

$$\begin{bmatrix}\dot{u}\\ \dot{w}\\ \dot{q}\\ \dot{\theta}\\ \dot{h}\end{bmatrix} = \begin{bmatrix}-0.08078 & 0.04174 & -0.03732 & -32.2 & 0\\ -0.22536 & -0.56292 & 276.5966 & 0 & 0\\ 4.2872e-5 & -7.155e-3 & -2.0775 & 0 & 0\\ 0 & 0 & 1 & 0 & 0\\ 0 & -1 & 0 & 287 & 0\end{bmatrix}\begin{bmatrix}u\\ w\\ q\\ \theta\\ h\end{bmatrix} + \begin{bmatrix}-0.04174\\ 0.56292\\ 7.155e-3\\ 0\\ 0\end{bmatrix} w_g$$

$$\begin{bmatrix}u\\ w\\ q\\ \theta\\ h\\ a_z\\ n_z\end{bmatrix} = \begin{bmatrix}1 & 0 & 0 & 0 & 0\\ 0 & 1 & 0 & 0 & 0\\ 0 & 0 & 1 & 0 & 0\\ 0 & 0 & 0 & 1 & 0\\ 0 & 0 & 0 & 0 & 1\\ -0.22536 & -0.56292 & -10.4034 & 0 & 0\\ 6.999e-3 & 0.017482 & 0.32309 & 0 & 0\end{bmatrix}\begin{bmatrix}u\\ w\\ q\\ \theta\\ h\end{bmatrix} + \begin{bmatrix}0\\ 0\\ 0\\ 0\\ 0\\ 0.56292\\ -0.017482\end{bmatrix} w_g \tag{14.111}$$

The next task is to define the state description of the appropriate white noise filter to produce normal velocity turbulence w_g as defined by equations (14.77), (14.78), and (14.104). With reference to Section 14.5.4, the turbulence scale length is given by $\mathscr{L}_w = h = 500$ ft and the aircraft velocity is $V_0 = 287$ ft/s; whence

$$K_{wg} = \sigma_{wg}\sqrt{\frac{\mathscr{L}_w}{\pi V_0}} = 0.7446\,\sigma_{wg}$$

$$T_{wg} = \frac{\mathscr{L}_w}{V_0} = 1.7422 \text{ s}$$

Let the rms turbulence intensity be $\sigma_{wg} = 1.0$ ft/s; then the filter transfer function as defined by equation (14.69) is

$$\frac{w_g(s)}{N(s)} = \frac{0.7446(1 + 3.0175\,s)}{(1+1.74222\,s)^2} \tag{14.112}$$

which has the time domain state description, described by equation (14.104),

$$\begin{bmatrix}\dot{w}_g\\ \dot{v}\end{bmatrix} = \begin{bmatrix}0 & 1\\ -0.32946 & -1.14797\end{bmatrix}\begin{bmatrix}w_g\\ v\end{bmatrix} + \begin{bmatrix}0.74024\\ -0.6045\end{bmatrix} N \tag{14.113}$$

where v is the dummy variable defined in equation (14.102). To complete the mathematical model building, it remains to augment the aircraft equations of motion (14.111) to include the

turbulence filter state equation (14.113), which results in the following state and output equations:

$$\begin{bmatrix} \dot{u} \\ \dot{w} \\ \dot{q} \\ \dot{\theta} \\ \dot{h} \\ \dot{w}_g \\ \dot{v} \end{bmatrix} = \begin{bmatrix} -0.08078 & 0.04174 & -0.03732 & -32.2 & 0 & -0.04174 & 0 \\ -0.22536 & -0.56292 & 276.5966 & 0 & 0 & 0.56292 & 0 \\ 4.2872e-5 & -7.155e-3 & -2.0775 & 0 & 0 & 7.155e-3 & 0 \\ 0 & 0 & 1 & 0 & 0 & 0 & 0 \\ 0 & -1 & 0 & 287 & 0 & 0 & 0 \\ 0 & 0 & 0 & 0 & 0 & 0 & 1 \\ 0 & 0 & 0 & 0 & 0 & -0.32946 & -1.14797 \end{bmatrix} \times \begin{bmatrix} u \\ w \\ q \\ \theta \\ h \\ w_g \\ v \end{bmatrix} + \begin{bmatrix} 0 \\ 0 \\ 0 \\ 0 \\ 0 \\ 0.74024 \\ -0.6045 \end{bmatrix} N$$

$$\begin{bmatrix} u \\ w \\ q \\ \theta \\ h \\ a_z \\ n_z \\ w_g \\ v \end{bmatrix} = \begin{bmatrix} 1 & 0 & 0 & 0 & 0 & 0 & 0 \\ 0 & 1 & 0 & 0 & 0 & 0 & 0 \\ 0 & 0 & 1 & 0 & 0 & 0 & 0 \\ 0 & 0 & 0 & 1 & 0 & 0 & 0 \\ 0 & 0 & 0 & 0 & 1 & 0 & 0 \\ -0.22536 & -0.56292 & -10.4034 & 0 & 0 & 0.56292 & 0 \\ 0.6998e-3 & 0.017482 & 0.323087 & 0 & 0 & -0.017482 & 0 \\ 0 & 0 & 0 & 0 & 0 & 1 & 0 \\ 0 & 0 & 0 & 0 & 0 & 0 & 1 \end{bmatrix} \times \begin{bmatrix} u \\ w \\ q \\ \theta \\ h \\ w_g \\ v \end{bmatrix} + \begin{bmatrix} 0 \\ 0 \\ 0 \\ 0 \\ 0 \\ 0 \\ 0 \\ 0 \\ 0 \end{bmatrix} N \tag{14.114}$$

Solution of equations (14.114) produces the transfer functions describing the aircraft response to filtered white noise when the rms turbulence intensity $\sigma_{wg} = 1.0$ ft/s. Transfer functions of immediate interest are

$$\frac{w(s)}{N(s)} = \frac{0.4167\, s(s^2 + 0.08364\, s + 0.0167)(s + 0.3313)(s + 5.607)}{s(s^2 + 0.06522\, s + 0.01667)(s+0.574)^2(s^2 + 2.648\, s + 3.1613)} \tag{14.115}$$

$$\frac{w_g(s)}{N(s)} = \frac{0.7402(s+0.3313)}{(s+0.574)^2} \tag{14.116}$$

$$\frac{n_z(s)}{N(s)} = \frac{-0.01294\, s^2(s^2+0.0733\, s+0.04752)(s+0.3313)(s+1.969)}{s(s^2+0.06522\, s+0.01667)(s+0.574)^2(s^2+2.648\, s+3.1613)}\ 1/\text{s} \tag{14.117}$$

The statistical properties of the response are quantified by the rms intensity σ for the turbulence input w_g of rms intensity σ_{wg}. Since the noise filter assumes an input rms intensity of $\sigma_{wg} = 1.0$ ft/s, the actual magnitude of the input turbulence intensity simply behaves as a scaling factor acting on the response transfer function of interest. The response turbulence intensity may therefore be calculated directly from the response transfer functions by calculating their variance σ^2, which is easily done using the statistical tools in MATLAB or Program CC.

Since, in accordance with the flying qualities requirements, the PSD of the input is assumed to have *cyclic frequency* dependency, the computed value of output variance must be factored by π as explained in Section 14.7.1. Accordingly, the computed variance of transfer function (14.115) is

$$\sigma_w^2 = 0.70435\ \text{ft}^2/\text{s}^2 \tag{14.118}$$

Whence rms output intensity per unit input intensity σ_{wg} is given by

$$\sigma_w = 0.8393\ \text{ft/s}$$

So, for example, a normal turbulence velocity disturbance of 15 ft/s intensity results in the aircraft normal rms velocity response intensity of 12.59 ft/s. This represents a modest attenuation much as might be expected from the F-104A at low speed on final approach to landing.

Consider now the filter transfer function (14.116) obtained in the general solution of equations (14.114). In the evaluation of the filter gain K_{wg}, output intensity was set at $\sigma_{wg} = 1.0$ ft/s; also, since the white noise input N has intensity $\sigma_N = 1.0$, the output variance is also unity. Calculation of the output variance of the filter transfer function (14.116) using either MATLAB or Program CC, when correctly factored by π, gives

$$\begin{aligned} \sigma_{wg}^2 &= 0.318194\pi = 0.999636\text{ft}^2/\text{s}^2 \\ \sigma_{wg} &= 0.9998\ \text{ft/s} \end{aligned} \tag{14.119}$$

Note that the variance σ_{wg}^2, and hence rms intensity σ_{wg}, is not exactly 1.0 since the limit of the numerical integration is not infinite but a suitably large number.

The computational tools available for the evaluation of the statistical properties of entire systems are extremely capable and versatile. In the present context the output variances of the example system defined by the state and output equations (14.114) may be evaluated simultaneously to give the row vector of variances:

$$\boldsymbol{\sigma}^2 = \begin{bmatrix} \sigma_u^2 & \sigma_w^2 & \sigma_q^2 & \sigma_\theta^2 & \sigma_h^2 & \sigma_{az}^2 & \sigma_{nz}^2 & \sigma_{wg}^2 & \sigma_v^2 \end{bmatrix}$$

Including the factor π, the numerical values of the variances are

$$\begin{aligned}\boldsymbol{\sigma}^2 = [&0.06281 \;\; 0.704355 \;\; 2.9634e-6 \;\; 4.491e-6 \;\; -6.624303e15 \\ &0.156638 \;\; 1.5107e-4 \;\; 0.999636 \;\; 0.747037]\end{aligned} \tag{14.120}$$

Thus the output variance of greatest interest in the present context is that for normal load factor response as defined by the transfer function (14.117). From equation (14.120),

$$\begin{aligned}\sigma_{nz}^2 &= 1.510727e-4 \\ \sigma_{nz} &= 0.0123\,\frac{\text{g}}{\text{ft/s}}\end{aligned} \tag{14.121}$$

From MIL-F-8785C, severe rms turbulence intensity at 500 ft is approximately $10 \sim 15$ ft/s, which results in a rms normal load factor response of $0.123 \sim 0.185\ g$. Again, this would seem reasonable for the F-104A on a low-speed approach to landing.

EXAMPLE 14.4

It is also instructive to review the magnitude of the aircraft frequency response to turbulence to gain an appreciation of the response spectrum and the degree of attenuation. This is most easily achieved using the reduced-order equations of motion. It is known that output attenuation increases with frequency beyond the natural bandwidth of the aircraft, and reduced-order modelling focuses on the short-period mode frequency region of the response spectrum. Since the degree of attenuation is determined in part by the system damping, the investigation of frequency response provides a means for interpreting the effectiveness of stability augmentation as a mechanism for improving ride quality.

Using the longitudinal model of the F-104A given in Example 14.3, the closed-loop state equation in (14.111) is reduced in order by removing the variables u, θ, and h. The output equation in (14.111) is also reduced in order to match, retaining only normal load factor n_z as an additional output variable. This reduces the system state-space description to a practical minimum format:

$$\begin{bmatrix}\dot{w}\\ \dot{q}\\ \dot{w}_g\\ \dot{v}\end{bmatrix} = \begin{bmatrix}-0.56292 & 276.5966 & 0.56292 & 0\\ -7.155e-3 & -2.077502 & 7.155e-3 & 0\\ 0 & 0 & 0 & 1\\ 0 & 0 & -0.32946 & -1.14797\end{bmatrix}\begin{bmatrix}w\\ q\\ w_g\\ v\end{bmatrix} + \begin{bmatrix}0\\ 0\\ 0.74024\\ -0.6045\end{bmatrix}N$$

$$\begin{bmatrix}w\\ q\\ w_g\\ v\\ n_z\end{bmatrix} = \begin{bmatrix}1 & 0 & 0 & 0\\ 0 & 1 & 0 & 0\\ 0 & 0 & 1 & 0\\ 0 & 0 & 0 & 1\\ 0.017482 & 0.323087 & -0.017482 & 0\end{bmatrix}\begin{bmatrix}w\\ q\\ w_g\\ v\end{bmatrix} + \begin{bmatrix}0\\ 0\\ 0\\ 0\\ 0\end{bmatrix}N \tag{14.122}$$

Equation (14.122) may be solved in the usual way to obtain the reduced order turbulence response transfer functions describing the response to white noise input N as follows:

$$\begin{aligned}
\frac{w(s)}{N(s)} &= \frac{0.4167(s+0.3313)(s+5.593)}{(s+0.574)^2(s^2+2.64\,s+3.147)} \\
\frac{q(s)}{N(s)} &= \frac{0.005296\,s(s+0.3313)}{(s+0.574)^2(s^2+2.64\,s+3.147)} \quad \frac{\text{rad/s}}{\text{ft/s}} \\
\frac{w_g(s)}{N(s)} &= \frac{0.7402(s+0.3313)(s^2+2.64\,s+3.147)}{(s+0.574)^2(s^2+2.64\,s+3.147)} = \frac{0.7402(s+0.3313)}{(s+0.574)^2} \\
\frac{v(s)}{N(s)} &= \frac{-0.6045(s+0.4034)(s^2+2.64\,s+3.147)}{(s+0.574)^2(s^2+2.64\,s+3.147)} = \frac{-0.6045(s+0.4034)}{(s+0.574)^2} \\
\frac{n_z(s)}{N(s)} &= \frac{-0.01294\,s(s+0.3313)(s+1.945)}{(s+0.574)^2(s^2+2.64\,s+3.147)} \quad 1/\text{s}
\end{aligned} \tag{14.123}$$

As before, w, q, and n_z describe aircraft response, and w_g and v describe the noise filter variables, where w_g is the effective aerodynamic input to the aircraft. Note also that the filter transfer functions simplify by cancellation to correctly represent the filter as originally defined in Example 14.3.

The frequency response of the reduced order system model (14.122) or of the individual transfer functions (14.123) can be obtained using MATLAB or Program CC; the magnitudes of the responses for the variables w_g, w, and n_z are shown in Fig. 14.10. The responses shown are essentially the Bode gain plots over a limited frequency range, chosen to reveal the high frequency properties of the reduced order model. When interpreting the responses, it is important to recall, from the characteristic polynomial of the transfer functions (14.123), that the short-period mode damping ratio is $\zeta_s = 0.744$, a relatively high value, and the frequency is $\omega_s = 1.774$ rad/s. These short-period mode properties clearly influence the shapes of the aircraft response to turbulence, as shown in Fig. 14.10.

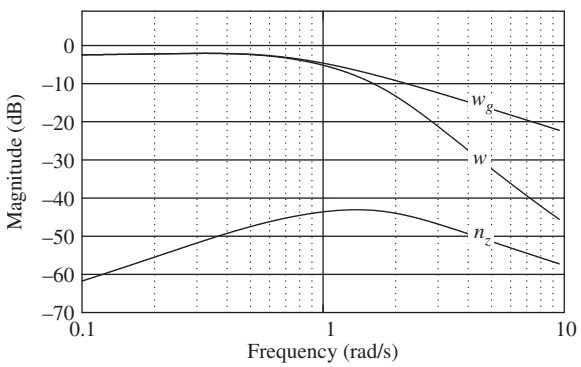

FIGURE 14.10 Longitudinal reduced-order frequency response of the Lockheed F104-A Starfighter for $\sigma_{wg} = 1$ ft/s.

The output of the filter w_g, when $\sigma_{wg} = 1$ ft/s, shows that the magnitude starts to "roll off" at a frequency a little below 1.0 rad/s and is otherwise unremarkable. The normal velocity w response of the aircraft follows the turbulence at low frequency with no significant attenuation, much as might be expected. Since the break frequency corresponds with the short-period mode frequency 1.774 rad/s, and since the system damping is very high, $\zeta_s = 0.744$, there is no visible peak in the response and it then "rolls off" very rapidly as frequency increases. The normal load factor n_z response shows a very high level of attenuation with a peak close to the short-period mode frequency. Bearing in mind that the aircraft is flying very slowly on approach, acceleration response to both control and external disturbances is subdued. At low frequency the response to turbulence is sufficiently slow and sufficiently well damped such that normal acceleration is not very perceptible. It is entirely consistent with the flight physics that the peak response in normal acceleration is at a frequency near the short-period mode, but as the mode damping is very high the response remains well attenuated. At higher frequency the magnitude of the normal load factor response "rolls off" much as expected.

The variances of the system variables in equations (14.122) were computed as described in Example 14.3 to give

$$\begin{aligned}\boldsymbol{\sigma}^2 &= \begin{bmatrix}\sigma_w^2 & \sigma_q^2 & \sigma_{wg}^2 & \sigma_v^2 & \sigma_{nz}^2\end{bmatrix} \\ &= \begin{bmatrix}0.6864063 & 2.856818e-6 & 0.9996355 & 0.7470366 & 1.541607e-4\end{bmatrix}\end{aligned} \tag{14.124}$$

These values compare well with those for the full-order system model in equation (14.120) and, correctly, the output variance of the turbulence filter is exactly the same.

The variance of normal load factor response, as defined by the reduced-order transfer function in (14.123), is given by the last term in the vector (14.124):

$$\begin{aligned}\sigma_{nz}^2 &= 1.51607e-4 \\ \sigma_{nz} &= 0.0123\,\frac{\text{g}}{\text{ft/s}}\end{aligned} \tag{14.125}$$

Whence, as in Example 14.3, at height 500 ft, for severe rms turbulence intensity of approximately $10 \sim 15$ ft/s, it is confirmed that this results in a rms normal load factor response intensity of $0.123 \sim 0.185\ g$.

References

Department of Defense (1980). *Military specification: Flying qualities of piloted airplanes.* Washington, DC: Department of Defense, MIL-F-8785C.

Department of Defense (1987). *Military standard: Flying qualities of piloted airplanes.* Washington, DC: Department of Defense, MIL-STD-1797A (USAF).

Gage, S. (2003). Creating a unified graphical wind turbulence model from multiple specifications. AIAA paper 20003-5529, *AIAA modeling and simulation technologies conference*, Austin, Texas.

Heffley, R. K., & Jewell, W. F. (1972). *Aircraft handling qualities data.* Washington, DC: National Aeronautics and Space Administration, NASA Contractor Report, NASA CR-2144.

Hoh, R. H., Mitchell, D. G., Ashkenas, I. L., Klein, R. H., Heffley, R. K., & Hodgkinson, J. (1982). *Proposed MIL standard and handbook: Flying qualities of air vehicles, Vol. 2: Proposed MIL handbook.* Wright-Patterson AFB, OH: Air Force Wright Aeronautical Laboratory, Technical Report AFWAL-TR-82-3081.

Jones, J. G. (1973). *Statistical discrete gust theory for aircraft loads: a progress report.* RAE Technical Report 73167, Royal Aircraft Establishment, Farnborough, Hampshire.

Ministry of Defence (2011). *Design and airworthiness requirements for service aircraft.* London: Ministry of Defence, Defence Standard 00-970/Issue 7, Part 1: *Fixed Wing*, Section 2: *Flight*.

Teper, G. L. (1969). *Aircraft stability and control data.* Hawthorne, CA: Systems Technology, Inc., STI Technical Report 176-1.

Thomasson, P. G. (2000). Equations of motion of a vehicle in a moving fluid. *AIAA Journal of Aircraft*, *37*(4), 630−639.